ÉCOLE DE TECHNOLOGIE SUPÉRIEURE
UNIVERSITÉ DU QUÉBEC

MANUSCRIPT-BASED THESIS PRESENTED TO
ÉCOLE DE TECHNOLOGIE SUPÉRIEURE

IN PARTIAL FULFILLEMENT OF THE REQUIREMENTS
FOR THE DEGREE OF DOCTOR OF PHILOSOPHY
Ph.D.

BY
Hassan RADVAR ESFAHLAN

FIXTURELESS GEOMETRIC INSPECTION OF NONRIGID PARTS USING "GENERALIZED NUMERICAL INSPECTION FIXTURE"

MONTREAL, FEBRUARY 10 2014

BOARD OF EXAMINERS

THIS THESIS HAS BEEN EVALUATED

BY THE FOLLOWING BOARD OF EXAMINERS

Mr. Souheil-Antoine Tahan, Thesis Supervisor
Mechanical Engineering Department at École de technologie supérieure

Mr. Louis Rivest, President of the Board of Examiners
Department of Automated Production Engineering at École de technologie supérieure

Mr. Victor Songmene, Member of the jury
Mechanical Engineering Department at École de technologie supérieure

Mr. René Mayer, External Evaluator
Mechanical Engineering Department at École Polytechnique

M. Jean-Christohpe Cuillière, Invited Evaluator
Mechanical Engineering Department at Université du Québec à Trois-Rivières

THIS THESIS WAS PRENSENTED AND DEFENDED

IN THE PRESENCE OF A BOARD OF EXAMINERS AND PUBLIC

JANUARY 15, 2014

AT ÉCOLE DE TECHNOLOGIE SUPÉRIEURE

ACKNOWLEDGMENT

I would like to express my deepest gratitude to my advisor Dr. Souheil-Antoine Tahan, professor in the department of Mechanical Engineering at the École de technologie supérieure for the years of support and encouragement of my academic work, for his trust, caring, patience, and for his for his countless contributions. Many thanks to the president and jury members of my PhD examination committee for reading my thesis and offering their valuable time and constructive feedback. I would like also to thank CRSNG for their financial support.

I would like to thank my wife Vajihe for her support and unwavering patience, my children Yashar and Yasmin providing me with unlimited happiness and pleasure.

Last but not least, I would like to thank my parents Hussein and Aghdas and my younger sister Lida, for their endless love, spiritual supports and many years of patience. A mere expression of gratitude clearly does not suffice.

For any errors or inadequacies that may remain in this work, the responsibility is entirely my own.

FIXTURELESS GEOMETRIC INSPECTION OF NONRIGID PARTS USING "GENERALIZED NUMERICAL INSPECTION FIXTURE"

Hassan RADVAR ESFAHLAN

RESUMÉ

Aujourd'hui les pièces mécaniques de forme libre et qui sont souples (non rigides) sont fréquentes dans les industries automobile et aéronautique. Ces pièces possèdent des formes significativement différentes à l'état libre que leurs formes nominales, telles que définies dans un modeleur numérique, en raison de leurs variations dimensionnelles et géométriques, l'effet de la gravité et les contraintes résiduelles induites par le procédé de fabrication. Pour l'inspection géométrique de ces pièces flexibles, des appareils d'inspection spécialisés tel que les gabarits de conformation, en combinaison avec les machines à mesure tridimensionnelle (MMT) et/ou des dispositifs d'acquisition de données optiques (scanners) sont utilisés. Ce qui se traduit immanquablement par des coûts et des délais additionnels qui se traduisent par une carence de compétitivité pour l'industrie.

L'objectif de cette thèse est de faciliter l'inspection dimensionnelle et géométrique des composants flexibles à partir d'un nuage de points sans l'aide d'un gabarit ou autre opération de conformation secondaire. Plus précisément, nous visons à développer une méthodologie pour localiser et quantifier les défauts de profil dans le cas des coques minces qui sont typiques pour les industries aéronautique et automobile.

La méthodologie présentée est basée sur le fait que la distance géodésique entre deux points d'une forme demeure invariante au cours d'une déformation isométrique (absence d'étirement, *stretch*). Cette étude développe donc la théorie générale, les méthodes et outils pour une métrologie des pièces non rigides en se basant sur l'hypothèse d'une déformation isométrique. Nous avons ainsi développé une méthode originale que nous avons nommée 'Gabarit d'Inspection Numérique Généralisée (GNIF)'. C'est une méthodologie robuste qui utilise les découvertes et technologies récemment développées en géométrie métrique et algorithmique. Les techniques de réduction dimensionnelle non linéaire sont employées pour

identifier les meilleures correspondances entre deux sets de points (CAD et nuage mesuré). Finalement, la méthode des éléments finis est employée en post-traitement pour ‘caler’ les deux nuages de points et produire un état numérique ‘virtuel’ d’une opération de conformation pour atteindre le but du projet qui est de *développer une approche générale de l'inspection géométrique sans gabarit pour les pièces non rigides*. La validation et l’exploration des performances métrologiques de notre approche sont réalisées sur des composants typiques de l’industrie.

Mots-clés: Inspection assistée par ordinateur, inspection géométrique; pièce flexible, calage nonrigid par éléments finis; distance géodésique, les techniques de réduction dimensionnelle non linéaire, calage.

FIXTURELESS GEOMETRIC INSPECTION OF NONRIGID PARTS USING "GENERALIZED NUMERICAL INSPECTION FIXTURE"

Hassan RADVAR ESFAHLAN

ABSTRACT

Free-form nonrigid parts form the substance of today's automotive and aerospace industries. These parts have different shapes in *free state* due to their dimensional and geometric variations, gravity and residual strains. For the geometric inspection of such compliant parts, *special inspection fixtures*, in combination with coordinate measuring systems (CMM) and/or optical data acquisition devices (scanners) are used. This inevitably causes additional costs and delays that result in a lack of competitiveness in the industry.

The goal of this thesis is to facilitate the dimensional and geometrical inspection of flexible components from a point cloud without using a jig or secondary conformation operation. More specifically, we aim to develop a methodology to localize and quantify the profile defects in the case of thin shells which are typical to the aerospace and automotive industries.

The presented methodology is based on the fact that the interpoint geodesic distance between any two points of a shape remains unchangeable during an isometric deformation. This study elaborates on the theory and general methods for the metrology of nonrigid parts. We have developed a *Generalized Numerical Inspection Fixture* (GNIF), a robust methodology which merges existing technologies in metric and computational geometry, nonlinear dimensionality reduction techniques, and finite element methods to introduce a general approach to the fixtureless geometrical inspection of nonrigid parts.

Keywords: Computer aided inspection; Geometric inspection; Compliant part; Nonrigid finite element registration; Geodesic distance; Nonlinear dimensionality reduction techniques, Registration

TABLE OF CONTENTS

Page

LIST OF TABLES

Page

LIST OF FIGURES

LIST OF ABREVIATIONS

y_i'	image of $x_i \mid x_i \in X$ in Y
σ	stress (loss function)
(X, d_X)	metric space where d is a metric on X
a_{ij}	ij^{th} element of matrix A
$dis\, f$	distortion of the map f
D_X	symmetric matrix of pair-wise geodesic distances. (For n points, it requires $\frac{n(n-1)}{2}$ calculations)
$d_X(a, b)$	distance between a pair of points
$\mathbb{R}^m$	m-dimensional Euclidean space
T	front propagation time
t_i	triangle index
$tr(V)$	Trace of matrix V
V^T	Transpose of matrix V
X, Y	surface
Y_M	space Y sampled by M points

LIST OF SYMBOLS

3D	Three-dimensional
ASME	American society of mechanical engineers
CAD	Computer aided design
CAI	Computer aided inspection
CAM	Computer aided manufacturing
CCA	Curvilinear component analysis
CF	Canonical form
CMM	Coordinate measuring machine
FEM	Finite element method
FMM	Fast marching method
FENR	Finite element nonrigid registration
GH	Gromov-Hausdorff
GMM	Gaussian mixture model
GNIF	Generalized numerical inspection fixture
H	Hausdorff
ICP	Iterative closest point
IDI	Iterative displacement inspection
ISO	International organization for standardization
ISOMAP	Isometric feature mapping
LMC	Least material condition
MDS	Multidimensional scaling

MMC	Maximum material condition
MVU	Maximum variance unfolding
NLDR	Nonlinear dimensionality reduction
NLM	Nonlinear mapping
PCA	Principal component analysis
RNIF	Robust numerical inspection fixture
SDT	Small displacement torsor
SM	Sammons's mapping
SMACOF	Scaling by majorizing a complicated function

INTRODUCTION

Thesis Problem Definition

This research targets the geometric inspection of a specific category of mechanical parts called nonrigid (or flexible). This kind of components is frequently used in automotive and aircraft construction (body, thin-walled parts, skin, etc.). For example, 37% of all car assembly stations are performed on flexible parts (Shiu, Ceglarek et al. 1997).

From solid mechanics we know that the mechanical behaviour of every part can be simulated as an ideal spring (or sets of ideal springs). On the other hand *Hook's Low* states that the force *F* needed to deform a spring by some distance *x* is proportional to that distance. By this definition, *stiffness* $k(=\frac{F}{x})$ is the *Load* divided by *Deformation*. Simply put, the stiffness is the amount of force needed to achieve a certain part deformation. While this description is very simplistic, the stiffness of any structure requires an exact definition of load configuration and the kind of metric used for measured deformation. The opposite concept of stiffness is *flexibility*. When said part A is more flexible than B, it means that A deforms more than B for a certain amount *F* applied in the same manner on both A and B. Thus *flexibility* is a relative notion. Indeed, asymptotically, all parts are flexible and conformable with some amount of force. In (Abenhaim, Desrochers et al. 2012) the authors suggest the following definition. If the application of the force 40 N[1] induces a distortion less than 5% of the allowable tolerance, then the component is classified as *rigid*. Therefore, a *flexible* part is a component where the application of the same force induces a displacement of more than 5% of the required tolerance.

Currently, a flexible workpiece must be constrained or clamped during the measurement process in order to simulate the *use state*[2] (Fig. 0.1 and 0.2). To that end, expensive and

---

[1] 40 N is widely used as the limit of acceptable force during manual assembly operations. The amount of force is justified by considerations of health and safety at work.

[2] Assembly conditions

special inspection fixtures (jigs) need to be designed and manufactured. On the other hand, some inspection stages cannot be fully automated with this conventional approach. As a result, the geometric inspection of flexible parts remains a time and money consuming process. Typically some inspection *set-up processes* for nonrigid parts in the aerospace industry require over 60 hours of operations[3]. On the other hand, even for simple parts, the quality of a planned inspection depends on the ability and experience of the operator.

Despite the multitude of papers and research that have been produced in the CAD, CAM and CAI fields, the inspection of flexible parts continues to pose difficulties and significant costs to industry because they need special fixation devices. This is also evidence of the lack of knowledge and theoretical foundations surrounding this special field. Thus, specific long-term goals must be set and systematically accomplished.

Figure 0.1 Inspection fixture for an aluminum part
(Ref. Bombardier Aerospace)

[3] Project's industrial partner (Bombardier Aerospace)

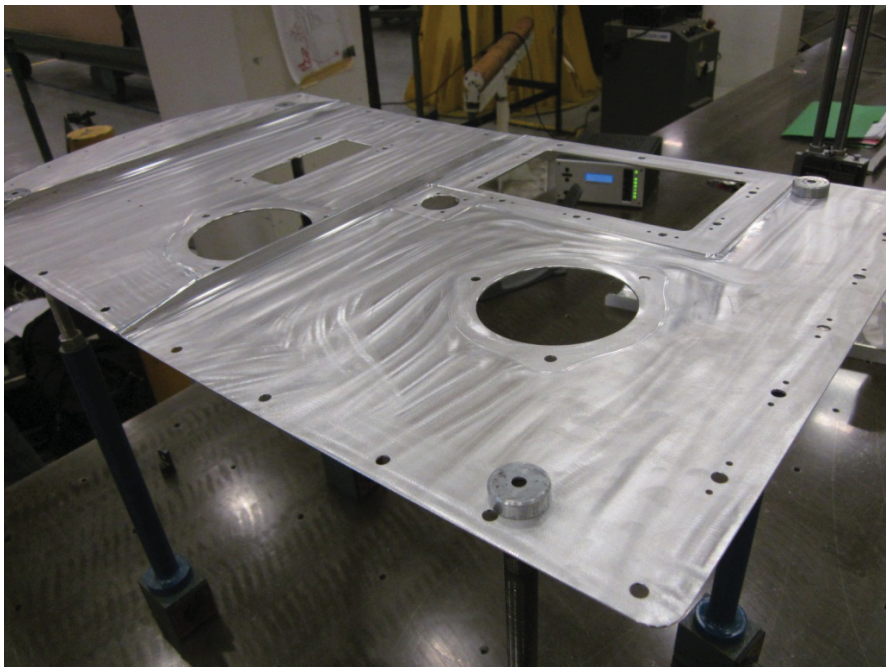

Figure 0.2 Aluminum part from the aerospace industry
(Ref. (Sabri, Tahan et al. 2013))

Geometric inspection, geometric modeling, range data acquisition and analysis have developed as separate fields of engineering among the various engineering and scientific communities. However, all these fields share common scientific concepts and there are many missed opportunities because of a lack of mutual connection and wasted synergy. Computer-Aided Inspection is one of these connection points, while nonrigid geometric inspection shares a profound degree of understanding with all the mentioned disciplines.

In this thesis we have developed *Generalized Numerical Inspection Fixture* (GNIF) and a more high-performing version named *Robust numerical inspection fixture* (RNIF) for an original and robust inspection methodology, one that brings together existing theories in Metric and Computational Geometry, Nonlinear Dimensionality Reduction Methods (NLDR), and Finite Element Analysis (FEM) to introduce a general approach to the fixtureless geometrical inspection of nonrigid parts.

Research Objectives

The aim of this thesis is to develop a holistic strategy in order to eliminate the use of inspection fixtures (jigs) and all constrain operations. To this end, the presented method has to be able to identify the actual geometric deviation (process error) from the defectless part with deformation (gravity, spring back, etc.). The amplitude and the location of profile defect should also be distinguished, with adequate accuracy[4], without any fixation device. Figure 0.3 demonstrate a simplified view of the inspection technique.

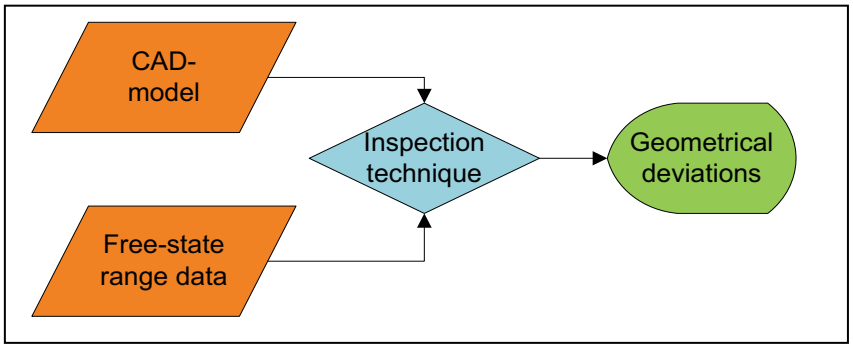

Figure 0.3 Simplified view of the inspection technique.

Note: For many industrial products it is possible to attribute some particular defects which are inherent to the process. This can be performed with prior knowledge of that product's manufacturing nature. As an example, unwanted shrinkage in some directions of moulded part, sand inclusion, pinhole, core shift, ram-off and other similar defects are, to some degree predictable as common foundry defects. Besides, if a causal mechanism which is related to each kind of defect can be recognized as priori, then a quantitative inspection of such defects can be automated. These kinds of surface defects can not only be recognized with *machine/computer vision* technologies, but can also be classified with *pattern recognition* methods. This study does not speak to these methods.

[4] Adequate precision is generally defined as $\leq 10 - 30\%$ of the permissible tolerance.

Thesis Organization

Our methodology was inspired by real industrial inspection processes. When we place the flexible part on the inspection fixture the prevailing idea is that we are going to simulate the use state. This is absolutely correct! But more specifically we can say that we are looking for some connection (correspondence) between distorted part and fixture, which in this thesis represents our CAD-model. *We present a methodology based on the fact that the interpoint shortest path (geodesic distance) between any two points on a shape remains unchanged during an isometric deformation. We call this property as* ***distance-preserving property of nonrigid parts***. In Figure 0.4, the CAD-model and range data are represented as a cantilever beam. For simplicity and without loss of generality, let's assume that some of prior information about boundary conditions is already known (e.g. support pint). Rigid registration (e.g., ICP based algorithm) can be done using this prior information. In the absence of plastic deformations, displacing x_1 to y_1 will deform the beam. This means that there will be a bijective (one-to-one correspondence) distance-preserving map between these two shapes (by bijective we do not mean the exact nodal correspondence). Also we assume that all pair-wise geodesic distances between the points on X (CAD-model) and Y (scanned data) are available (e.g., using fast marching). If we can introduce a similarity measure in order to find a correspondence between these two metric spaces, the step that we call *finite element nonrigid registration* (FENR) can be performed: (a) Find the correspondence (e.g. y_1 is the image of x_1). (b) Knowing that some boundary conditions such as prior information apply, find the the best correspondence then displace x_1 towards y_1. (c) Calculate the geometric deviation between the deformed CAD-model and measure range data. Based on the FENR approach, two methodologies were developed and tested (Radvar-Esfahlan and Tahan 2011, Radvar-Esfahlan and Tahan 2011).

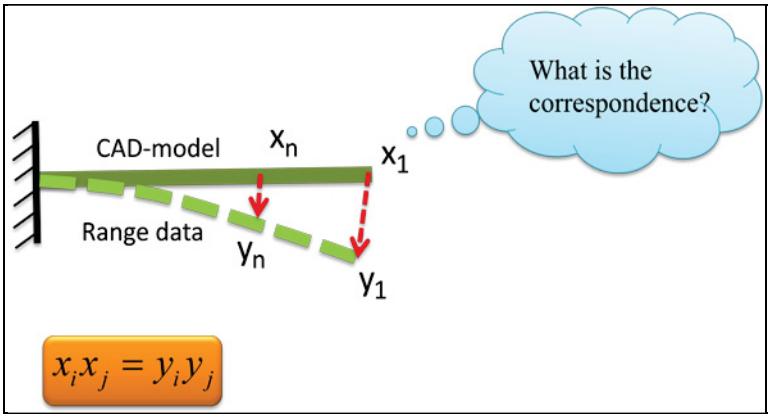

Figure 0.4 Finite Element Nonrigid Registration (FENR)

The content of this thesis consists of three chapters. The aim of Chapter 1 is to construct a solid frame work in order to uncover a unique horizon along with new metrological definitions such as *distance preserving property of nonrigid parts* and *finite element nonrigid registration.* For the first time in dimensional metrology we will construct a theoretical foundation which will brings together certain existing technologies from different domains in Chapter 1. In brief, we will seek out geometric properties that are invariant to elastic deformations. In Chapter 2 we will try to robustify the GNIF technique by filtering some incoherent geodesics out of similarity detection algorithm. In Chapter 3 we will present a systematic comparison of some well-known dimensionality reduction techniques in order to evaluate their accuracy and potential for non-rigid metrology. Chapter 3 looks at the potential, precision and accuracy of nonlinear dimensionality reduction methods. What's more, the content of this chapter paves the way for future research. Figure 0.5 provides a quick snapshot of the thesis organization.

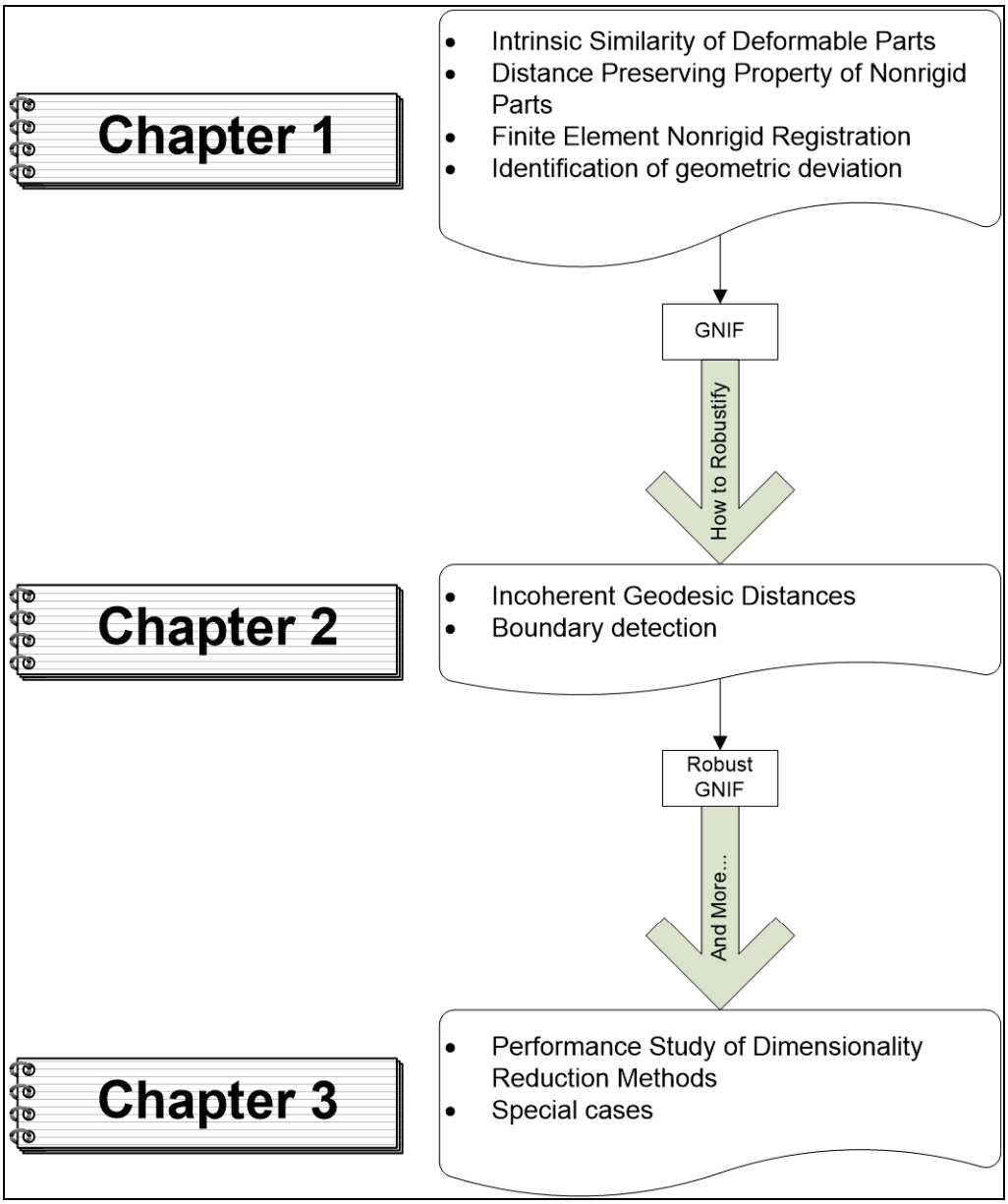

Figure 0.5 Fixtureless geometric inspection of nonrigid parts using GNIF

REVIEW OF PREVIOUS RESEARCH

Geometric inspection of flexible parts using range data

Non-contact 3D digitizing systems exposed a new perspective in the geometric inspection of both rigid and nonrigid parts because they can handle a huge number of range data in seconds whereas using traditional touch probes is a time-consuming process. These systems are suitable for the fast and contact free measurement of parts without clamping. In the case of flexible materials this contactless measurement capability is very important. Bibliographical research demonstrates that -in the field of nonrigid inspection- there are only three distinguished studies.

Weckenmann and Gabbia (Weckenmann and Gabbia 2005) proposed a measurement method using *virtual distortion compensation*. They used measurement results to extract object features like holes or edges. After the feature extraction process, they transformed the range data into a finite element analysable CAD-model. Then using some prior information about boundary conditions they gradually transformed the modeled range data into a CAD-model. Their method was not completely automated because their suggested method needed some human challenges to identify the correlation between certain special points like holes and assembly joint positions. For each part, the reverse engineering process had to be performed. Transforming the point cloud to a computer aided analyzable model is a highly time-consuming process. Besides, transforming each range data into CAD-model can introduce a geometric defect caused by the modeling process. On the other hand we know that, a FEM mesh created from a CAD-model provides more precise results than a triangle mesh from a measurement result. Finally, it seems that this method is not suitable for really flexible parts because the effect of gravity and the 3D scanning position of the part have not been taken into consideration.

The concept of the *Small Displacement Torsor* (SDT) has been developed by Bourdet and Clément (Bourdet and Clément 1976) to solve the general problem of rigid surface registration using rigid body movements. Lartigue *et al.* (Lartigue, Theibaut et al. 2006) took advantage of the possibilities offered by voxel representation and SDT methods for the

dimensional metrology of flexible parts. This time, they considered the effects of gravity and spatial situation of a scanned part. The method is fundamentally based on finding the correspondence between the measured range data and the CAD-model. They simulated the use state and knowing some prior information about the inspection process they deformed the CAD-model in order to measure the real geometric deviation. They did not consider the effect of spring back which is the inseparable part of majority of mechanical products. On the other hand, the SDT is more suitable for the small deformations. More accurate results can even be achieved if one considers the effect of material flexibility.

Abenhaim, Tahan *et al.* (Abenhaim, Tahan et al. 2011) developed an *iterative displacement inspection* (IDI) which smoothly deformed the CAD mesh data until it matched the range data. Their method was based on optimal step nonrigid ICP algorithms (Amberg, Romdhani et al. 2007). The proposed IDI method had some limitations. Their method was not tested in non-continuous areas such as holes, and the point cloud needed to be dense enough because the method's similarity measure was only based on nearest distance calculation. The major flaw of this method was hidden in the fact that it strongly depended on finding some trials and prior flexibility parameters which would vary depending on thickness (local rigidity of the part).

Recently, in (Jaramillo, Prieto et al. 2013, Jaramillo, Prieto et al. 2013) the authors proposed a methodology that used the partial range captures of the workpiece. The inspection process was based on an iterative nonrigid alignment algorithm. To this end, a transformation to the CAD model was applied at each iteration which was calculated by minimizing the error with a partial-view model. By this method it was assumed that the acquired region contains sufficient feature points that would enable model alignment. We underline that the ability of partial inspection is one of the capabilities of the GNIF technique first presented in (Radvar-Esfahlan and Tahan 2011).

While previously mentioned methods seek a quantitative analysis of nonrigid parts (geometric deviation), qualitative visual inspection of these parts using light-reflection patterns werefirst introduced by Gentilini and Shimada (Gentilini and Shimada 2011). Although the accuracy of their method was acceptable (0.3-0.6mm) for average industrial

applications, those kinds of defects are widely traceable with *machine/computer vision* technologies.

The drawback of all these studies is that the aforementioned methods have limited industrial applications. As a result, nowadays in industry the only way for the geometric inspection of flexible parts is to use high cost inspection fixtures. In this research we will try to construct a solid theoretical framework to handle fixtureless nonrigid geometric inspection.

Rigid and nonrigid surface registration

In tandem with mechanical engineers but in different fields like *Computer Vision*, *Biomedical Engineering* and *Pattern Recognition,* much research has been done on rigid and nonrigid registration, as well as deformable surface comparison. Besl and McKay (Besl and McKay 1992) developed the *Iterative Closest Point* (ICP) algorithm. ICP is an iterative method for the rigid registration of 3D shapes. The ICP algorithm is one of the common techniques for 3D rigid surface registration. Suppose that we are given two shapes X and Y. The goal of ICP is to find the rigid transformation which brings two shapes as close as possible. The closeness is measured by the Hausdorff distance between two shapes. Many versions of ICP have been proposed. They differ from the selection and matching of points, to the minimization strategy(Bentley 1975, Greenspan and Godin 2001). We refer the reader to (Rusinkiewicz and Levoy 2001) for an account and comparison between some ICP variants.

Myronenko, Song *et al.* (Myronenko, Song et al. 2007) introduced a probabilistic method for rigid, affine, and nonrigid point set registration, called the *Coherent Point Drift algorithm*. They considered the alignment of two point sets as the probability density estimation, where one point set represents the *Gaussian Mixture Model* centroid, and the other represents the data point. They iteratively fitted the GMM centroids by maximizing the likelihood and found the posterior probabilities of centroids, which provide the correspondence probability. The method based on forcing the GMM centroids to move coherently as a group, preserved the topological structure of the point sets. The convergence of presented method when there is no exact nodal correspondence between two range data sets is under question.

Schwartz, Shaw *et al.* (Schwartz, Shaw et al. 1989) were the first to use the *Multidimensional Scaling* (MDS) method. They flattened the convoluted surfaces of the human brains in order to compare them to each other in order to study the functional architectures of the brain. For some, their work was a breakthrough in which surface geometry was translated into a plane. They presented an iterative method in which they gradually decreased the dimension of a multidimensional space. In our knowledge of differential geometry, the Gaussian curvature is an intrinsic invariant of the surfaces. For example, a sphere and a flat surface cannot be mapped into each other without distortion. As a result of plane restriction, their presented method was not capable of properly matching convoluted surfaces. The *stress* and the *goodness of fit* used in the mentioned paper have been historically proposed by Kruskal (Kruskal 1964). Zero Stress means perfect Goodness of fit, in other words, there is a perfect relationship between similarity and interpoint distance. From the first generation of MDS until now, many variants of minimization algorithms have been created to minimize *stress* function. One of the most straightforward and successful among them was developed by De Leeuw (De Leeuw 2005). SMACOF (scaling by majorizing a complicated function) to minimize a complicated function $p(x)$ (e.g. stress function), constructs a quadratic function $q(x,y)$ in such a way that the constructed function is always above the complicated function except for one coincidence point. In each iteration with initial value x_0 , $q(x, x_0)$ it is minimized to find x_1. In the next iteration $q(x, x_1)$ is minimized. The iteration continues until convergence.

The *Fast marching method* was introduced by Sethian (Sethian 1996). It is like a *Dijksta algorithm* in discrete domains which solves the *Eikonal equation* in order to compute the geodesic distance on range surfaces. The only difference with the Dijkstra algorithm is in the updating process. The fast marching method was extended to triangulated surfaces by Kimmel and Sethian (Kimmel and Sethian 1998). Vast ranges of FMM applications in geometry, grid generation, image enhancement and noise removal, shape detection and recognition, CAD and computational geometry as well as other applications in optimal path planning, etching and deposition in microchip fabrication have been discussed in (Sethian 1999). In fact, Sethian was the first to introduce a solid framework in order to solve the boundary value problem without iteration.

Elbaz and Kimmel (Elbaz and Kimmel 2003) presented a blend of topology and statistical methods, to introduce the concept of *Invariant signature* for surfaces. Their method was based on fast marching on a triangulated domain algorithm followed by an MDS technique. They have practically transformed the problem of matching isometric-nonrigid surfaces into the problem of rigid surface matching. Using MDS, they embedded surfaces X and Y into some common embedding spaces Z called *Canonical form* and then measured the similarities using the *Hausdorff distance*. Their method is strongly based on the Kimmel and Sethian (Kimmel and Sethian 1998) method in wich computing the geodesic distance is done on triangular meshes. As the nature of their study was based on classification and pattern recognition, the accuracy of their presented method as a measure metric space similarity was not discussed. On the other hand the uncertainty of canonical forms as a result of geodesics by means of fast marching method, as well as the uncertainty related to the least square multidimensional scaling process should be investigated in depth. In this particular project, the similarity measure plays a critical role in the accuracy of canonical forms where of nonrigid inspection will be considered using typical mechanical engineering case studies.

In spite of the canonical forms in which two metric spaces are mapped into acommon space, Bronstein *et al.* (Bronstein, Bronstein et al. 2006) proposed a method which mapped two metric shapes directly into each other. Despite classic MDS here the distortion was a kind of similarity measure. The distortion showed that in which degree two shapes are similar (or dissimilar). Other advantages of their method are the ability to measure the similarity of shapes in which there is no exact nodal correspondence between range data sets. The presented method was also suitable in the case of partial matching.

Nonlinear dimensionality reduction

Dimensionality reduction is the meaningful transformation of high dimensional data into low dimensional space by minimizing information loss. *Principal Component Analysis* (PCA) (Jolliffe 2005) is the most traditional linear dimensionality reduction method which maximizes the variance preservation. However this linear technique along with other linear methods cannot handle complex nonlinear data. This is why nonlinear dimensionality reduction techniques are at the core of most research. A large number of nonlinear techniques

have been developed in the last decades (Maimon and Rokach 2005, Lee and Verleysen 2007).

Any manifold can be fully described by a matrix of interpoint distances. This can simply be done by means of a graph based on distance calculation methods. In many applications, like in our particular case, the distance remains unchangeable during manifold deformation. In this case, geodesics instead of Euclidean distance can be used. In the previous section we reviewed one of the distance-preserving dimensionality reduction methods. In fact, distance preservation is one of the first criteria to be used for dimensionality reduction. There are also other kinds of nonlinear dimensionality reduction (NLDR) methods.

In (Sammon Jr 1969) Sammon mapped an N, L-dimensional space into a lower dimensional space in such a way that the inherent structure of the higher space was preserved, all the while mapping into the lower space. The idea behind Sammon's NLM is to try to approximately preserve the pairwise distance in two higher and lower spaces. To this end the author used the same idea as MDS. Sammon's NLM first defines an error parameter and then uses the steepest descent procedure to try to minimize error function. The NLM algorithm does not need any prior information about the data except that the number of iterations should be set before iteration. It is also an efficient algorithm when dealing with hyper-spherical and hyper-ellipsoidal data structures. In spite of these advantages, the output scatter diagram of NLM can be confusing when dealing with high dimensional data structures. On the other hand, it is incapable of handling a large number of data vectors. To this end, the author proposes a data compression technique in order to reduce the larger data sets. Many variants of NLM which differ in optimization techniques are presented by other researchers. For instance, Mao and Jain (Mao and Jain 2002) presented the SAMANN (Sammon's artificial neural network) method, which instead of classical optimization techniques (i.e. steepest descent), uses modern methods of optimization (i.e. neural network based methods).

Other variants of MDS and NLM are presented by Demartines and Hérault (Demartines and Hérault 1997). The CCA (curvilinear component analysis) minimizes the same error/stress function, based on pairwise distance in both higher and lower data structure as in MDS and NLM. However, it is closely related to Kohenon's self organizing map (SOM) (Kohonen

1982). Inother words, it borrows both the idea of multivariate data analysis and the principals of the SOM method. It has all the advantages of previously mentioned methods, however in spite of the SOM in which a high dimensional data structure was mapped into a fixed lattice; CCA maps it into a continuous space in order to take the shape of a high-dimensional manifold. CCA performs two tasks, vector quantization of higher data set followed by the nonlinear projection of these quantizing vectors toward a lower dimensional space. In comparison to previously reviewed methods, CCA converges very fast.

In addition to distance preserving techniques, topology preserving methods are another class of dimensionality reduction techniques that tend to preserve important data structures in the geometric mapping structure. One simple example of topology preserving maps is a Mercator projection of the earth into 2D space. While this kind of mapping gives invaluable visual information, distortion can't be prevented in some areas. Locally linear embedding (Roweis and Saul 2000) is an eigenvector based technique (like PCA and MDS) where optimization doesn't involve local minima and iterative optimizations. It tries to preserve the local angles. LLE supposes that each point with its neighbors on the manifold lies on, or close to, a locally linear patch. Then it tries to characterize the local geometry of the patches by finding linear coefficients that reconstruct each point by using its *k*-nearest neighbors.

State of the art summary

Rigid and Nonrigid surface registration, Nonlinear Dimensionality Reduction and Geometric inspection of flexible parts using range data have developed as separate fields of engineering among the various engineering and scientific communities. However, all these fields share common scientific concepts, and there are many missed opportunities because of a lack of mutual connection and wasted synergy. Computer-Aided Inspection is one of these connection points, while nonrigid geometric inspection shares a profound degree of understanding of all the mentioned disciplines. While in the last decade a variety of papers have been published on Rigid and Nonrigid surface Registration and Dimensionality reduction methods, this volume of publication does not compare to the number of research on the nonrigid inspection of flexible (deformable) parts. As a result, the inspection of flexible

parts continues to pose difficulties and imposes significant costs on industry because of the need for special fixation devices.

CHAPITRE 1

NONRIGID GEOMETRIC METROLOGY USING GENERALIZED NUMERICAL INSPECTION FIXTURES

Hassan RADVAR-ESFAHLAN ; Souheil-Antoine TAHAN

Laboratoire d'ingénierie des produits, procédés et systèmes (LIPPS)

École de Technologie Supérieure

Montréal, Canada, H3C 1K3

Article published in « *Precision Engineering* », Volume 36, Issue 1, Pages 1-9 (January 2012)

1.1 Abstract

Freeform surfaces have become an integral part of the automobile and aerospace industries. The parts with a very thin wall in proportion to their size are referred to as nonrigid (or flexible) parts. Generally, for the geometric inspection of such flexible parts, *special inspection fixtures,* in combination with coordinate measuring systems (CMM), are used because these parts may have different shapes in a *free state* from the design model due to dimensional and geometric variations, gravity loads and residual strains. A general procedure to eliminate the use of inspection fixtures will be developed. Presented methodology is based on the fact that the interpoint geodesic distance between any two points of a shape remains unchangeable during isometric deformation. This study elaborates on the theory and general methods for the metrology of nonrigid parts. We will merge existing technologies in metric and computational geometry, statistics, and finite element method to develop a general approach to the geometrical inspection of nonrigid parts.

Keywords: Geometric inspection; Compliant part; Intrinsic geometry; Geodesic distance; Nonrigid registration; Multidimensional scaling

1.2 Introductoin

It is clear that quality product control is essential to company survival in a competitive market. With *computer-aided inspection* (CAI), raw data from a 3D scanner or CMM can be compared to the original CAD design to generate impressive inspection reports. Generally, for the geometric inspection of nonrigid parts, *inspection fixtures,* in combination with coordinate measuring systems (CMM), are used. The aim of this study is to develop new methodology to eliminate the use of inspection fixtures. Three-dimensional optical digitizing systems are suitable for the measurement of large-sized flexible parts for they allow non-contact measurement and are able to deliver, in a relatively short time, large clouds of points that are representative of object surfaces. The part is setup on a portable 3D optical digitizing system which is installed in a production line regardless of datum shown in the engineering drawings. Due to weight, and of course supports, part deformations occur. An identification method must be defined in order to extract geometrical profile deviations due to manufacturing defects while simulating the *use state* to compensate for a spring-back effect and gravity.

In many cases, it is possible to associate specific products, materials, and manufacturing processes with particular types of seeable surface defects. For instance, injection-moulded components may tend to present undesired sink. Similarly, cutting, grinding, and polishing operations may produce characteristic surface markings, including an altered texture and excessive burrs due to tool wear or the inclusion of foreign abrasive materials. It is important to appreciate that in each case, in addition to possible surface discoloration, these defects tend to induce a deviation in the component's surface shape away from a nominal form. The nature of this deviation, or the type of expected defect, is often somewhat predictable. If in addition, a causal mechanism can be identified, then a quantitative analysis of such defects may be used as a basis for automatic process control. These surface defects can be recognized with machine vision technologies. They can also be classified with pattern recognition methods. This study does not address these methods.

The remainder of this paper presents the theory and methods for geometric inspection in nonrigid parts. Section 2 provides a comprehensive literature review of the necessary fields. Section 3 gives theoretical foundations in metric and discrete geometry as well as fast marching method and multidimensional scaling. In section 4 we introduce the methodology to measure the geometric deviation of nonrigid bodies. Section 5 gives verification and validation of these methods using four case studies. Section 6 presents conclusions.

1.3 Prior Work

1.3.1 Geometric inspection of solid and flexible parts

Non-contact 3D digitizing systems exposed a new horizon in industrial inspection of both rigid and nonrigid parts because they deliver much more data than mechanical probes, in a shorter time. A state of the art review of the most important measuring techniques is presented in (Savio, De Chiffre et al. 2007) along with their capacity for freeform measuring tasks. Throughout these presented methods (Li and Gu 2004, Li and Gu 2005, Gao, Gindy et al. 2006, Shi and Xi 2008), the manufactured part is assumed to have a similar shape to the CAD model, allowing for comparison. All presented methods, and most recently Ravishankar, *et al.* (Ravishankar, Dutt et al. 2010), have used rigid registration as similarity measures.

Weckenmann and Gabbia (Weckenmann and Gabbia 2005) proposed a measuring method using virtual distortion compensation. They used the measurement results to extract object features like holes or edges. Some of these were relevant to the assembly process; others were subject to further inspection. From the information about the transformation of assembly features from their actual to their nominal position, virtual distortion compensation was used to calculate feature parameters of the distortion compensated shape. Their method was not completely automated because the suggested method needed some human challenges to identify the correlation between some special points like holes and assembly joint positions. These led the controller to find the boundary conditions of the FEM problematic. Besides, transforming the point cloud to a computer-aided analyzable model is a very time

consuming process. These drawbacks then largely improved in (Weckenmann, Weickmann et al. 2007). To this end they deformed CAD-model and mapped it towards range data. By this way, they decreased the time of inspection. A FEM-mesh created from a CAD-model, also provided more precise results than a triangle mesh from measurement results. However, proposed method still needed human intervention in order to find the correspondence between CAD-model and range data.

The concept of the *Small Displacement Torsor* (SDT) was developed by Bourdet and Clément (Bourdet and Clément 1976) to solve the general problem of a geometrical surface model fit to a set of points using rigid body movements. Lartigue *et al.* (Lartigue, Theibaut et al. 2006) took advantage of the possibilities offered by voxel representation and SDT method for the dimensional metrology of flexible parts. This time, they considered the effect of gravity and the spatial location of a scanned part. This method is fundamentally based on finding the correspondence between the cloud of all measured points and CAD meshed data. In fact, the SDT is more suitable for small deformations.

Abenhaim *et al.* (Abenhaim, Tahan et al. 2011) developed an *Iterative Displacement Inspection* (IDI) which smoothly deformed the CAD mesh data until it matched the range data. Their method was based on optimal step nonrigid ICP algorithms (Amberg, Romdhani et al. 2007). The point cloud needs to be dense enough because the method's similarity measure is based on the nearest distance calculation. The method depends on finding some flexibility parameters which could vary according to thickness. The mentioned drawbacks cause previously mentioned methods to limit their applicability in industrial applications.

1.3.2 Rigid and nonrigid surface registration

Besl and Mckay (Besl and McKay 1992) developed an iterative method for the rigid registration of 3D shapes. The ICP algorithm is one of the common techniques for the refinement of partial 3D surfaces (or models) and many variant techniques have been investigated (Bentley 1975, Rusinkiewicz and Levoy 2001). Shi *et al.* (Shi, Xi et al.) pointed out that ICP-based algorithms may not fit inspection applications because the transformation

matrix for registration is estimated in a way that total shape error is minimized. This cannot be applied to industrial quality control. Myronenko and Song (Myronenko, Song et al. 2007) introduced a probabilistic method for rigid, affine and nonrigid point set registration, called the Coherent Point Drift algorithm. They considered the alignment of two point sets as the probability density estimation, where one point set represents the Gaussian Mixture Model centroid, and the other represents the data point. They iteratively fitted the GMM centroids by maximizing the likelihood and found the posterior probabilities of centroids, which provide the correspondence probability. The method based on forcing the GMM centroids to move coherently as a group preserved the topological structure of the point sets.

The *Fast Marching Method* was introduced by Sethian (Sethian 1996, Sethian 1999, Sethian 2008) as a computationally efficient solution to *Eikonal equations* on flat domains. The fast marching method was extended to triangulated surfaces by Kimmel and Sethian (Kimmel and Sethian 1998). The extended method solved the Eikonal equation on flat rectangular, or curved triangulated, domains. Elad and Kimmel (Elad and Kimmel 2003) presented the concept of *Invariant Signature* for surfaces. Their method used fast marching on triangulated domains followed by *Multidimensional Scaling* (MDS) technique. They practically transformed the problem of isometric-nonrigid surface matching into a matching of rigid surfaces problem. Using MDS, they embedded surfaces X and Y into some common embedding space Z called *Canonical form* and then measured their similarity using the *Hausdorff distance*. Their method is strongly based on the Kimmel and Sethian (Kimmel and Sethian 1998) method in computing the geodesic distance on triangular meshes. In fact, Euclidean embedding is rarely without distortion. Cox and Cox (Cox 2000) showed how points of a configuration from non-metric MDS can be forced to lie on the surface of a sphere. Bronstein *et al.* (Bronstein, Bronstein et al. 2006, Bronstein, Bronstein et al. 2007) proposed a method: instead of embedding X and Y into some common embedding space Z that introduced inevitable distortions, they embedded X directly into Y. In spite of the Elad and Kimmel (Elad and Kimmel 2003) method, they did not use canonical forms anymore and the distance between two surfaces was obtained from the solution of the embedding problem itself.

1.4 Theoretical Foundations

1.4.1 Metric spaces

Let X and Y be metric spaces and $f: X \to Y$ an arbitrary map. The *distortion* of f is defined by:

$$\text{dis } f = \sup_{a.b \in X} \left| d_Y(f(a), f(b)) - d_X(a,b) \right| \tag{1}$$

The distance $d_X(a,b)$ between a pair of points in X is mapped to the distance $d_Y(f(a), f(b))$ between the images of a and b under f. For a complete *Riemannian manifold*, the metric $d(a,b)$ is defined as the length of the shortest curve (*geodesic*) between a and b (Burago, Burago et al. 2001).We denote X and Y as subsets of a metric space (Z,d_Z). The *Hausdorff distance* between X and Y, $d_H(X, Y)$, is defined by:

$$d_H(X,Y) = \max\left(\sup_{x \in X} \inf_{y \in Y} d_Z(x,y), \sup_{y \in Y} \inf_{x \in X} d_Z(x,y) \right) \tag{2}$$

and *Gromov-Hausdorff* distance between two metric spaces (X, dx) and (Y, dy) is defined as:

$$d_{GH}(X,Y) = \inf_{Z,f,g} \left(d_H^Z(f(X), g(Y)) \right) \tag{3}$$

where $f: X \to Z$ and $g: Y \to Z$ are isometric embeddings (distance preserving) into the metric space (Z,d) . With computational perspective one can say:

$$\boxed{\begin{array}{ccc} (X, d_X) & \xleftarrow{d_{GH}} & (Y, d_Y) \\ f \downarrow & & g \downarrow \\ (f(X), d) & \xleftarrow{d_H^Z} & (g(Y), d) \end{array}} \tag{4}$$

d_{GH} satisfies the triangle inequality, i.e. ,

$$d_{GH}(X_1, X_3) \le d_{GH}(X_1, X_2) + d_{GH}(X_2, X_3) \tag{5}$$

for any metric spaces X_1 , X_2 , X_3. Moreover $d_{GH}(X, Y) = 0$ if and only if X and Y are isometric. Now for functions $\varphi: X \to Y$ and $\psi: Y \to X$ consider the numbers

$$A(\varphi) := \sup_{x_1, x_2 \in X} \left| d_X(x_1, x_2) - d_Y(\varphi(x_1), \varphi(x_2)) \right|,$$

$$B(\psi) := \sup_{y_1, y_2 \in Y} \left| d_X(\psi(y_1), \psi(y_2)) - d_Y(y_1, y_2) \right|,$$

$$C(\varphi, \psi) := \sup_{x \in X, y \in Y} \left| d_X(x, \psi(y)) - d_Y(\varphi(X), y) \right|$$

Then d_{GH} can be written as:

$$d_{GH}(X,Y) = \inf_{\substack{\varphi:X\to Y \\ \psi:Y\to X}} \frac{1}{2}\max\left((A(\varphi),B(\psi),C(\varphi,\psi)\right) \tag{6}$$

This expression is the main idea behind the computational approaches in (Bronstein, Bronstein et al. 2006) and (Mémoli and Sapiro 2005) and is the alternative formulation of (3) which is computationally tractable. The main difference between GH and ICP distances lies in that while the former only looks at the interpoint distance between points on each shape, without any regard for the ambient space, the latter requires finding a Euclidean isometry that aligns the shapes. Mémoli (Mémoli 2008) proved that Euclidean distance admits the GH distance as upper bound, more precisely that, for some constants c>0, $d_{ICP} \le c.(d_{GH})^{1/2}$.

1.4.2 The fast marching method on range data

The notion of *geodesic distance* was originally defined as the length of a geodesic path, where the geodesic path between two points on the surface of the Earth is considered the *shortest path* since one is constrained to travel on the Earth's surface. The concept of geodesic distance can generalized to any mathematical surface, and defined as the length of the shortest path between two points that lie on a surface, when the path is constrained to lie on the surface. The first and most important of our approaches is to approximate the geodesic distance between all range data. If the sampling domain is dense enough, one idea is to approximate the geodesic distance between points with the famous *Dijkstra's shortest path algorithm* (Dijkstra 1959); but the shortest path computed by Dijkstra's algorithm does not always lead to the real shortest path. This inconsistency is due to the fact that we are allowed to move in the graph using only nodal points. *Fast marching method* (FMM) (Sethian 1996, Sethian 1999, Sethian 2008) is a numerical algorithm for solving an *Eikonal equation* on a rectangular orthogonal mesh. Later on, Kimmel and Sethian (Kimmel and Sethian 1998) extended the fast marching method to triangulated domains with the same computational complexity. The standard methods for the boundary value view require iteration. Sethian described FMM as a method which allows one to solve the boundary value problem without iteration. Technically, it is a dynamic programming sequential estimation method, very

similar to Dijkstra's algorithm. We refer the reader to (Sethian 1999, Bronstein, Bronstein et al. 2007) for an account. In this way, we are going to compute the geodesic distance between one vertex and the rest of the surface vertices.

1.4.3 Isometric embedding

In order to compare the nonrigid shapes we should look at their intrinsic geometries because they rest unchanged during isometric deformations. Consider X and Y as two metric shapes (Fig. 1.1).

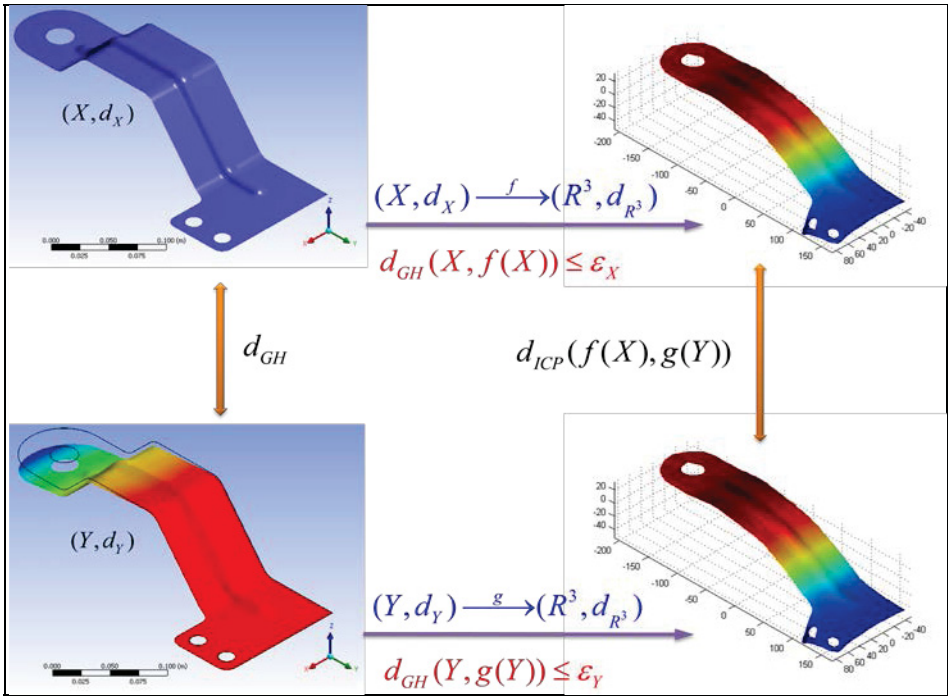

Figure 1.1 Canonical form distance

Let us compute the *Canonical Form* (CF) as:

$$\begin{aligned} f &= \arg\min_{f:X\to\square} dis\, f \quad \to \quad Z(X) = f(X) \\ g &= \arg\min_{g:Y\to\square} dis\, g \quad \to \quad Z(Y) = g(Y) \end{aligned} \tag{7}$$

and compare the extrinsic geometries of canonical forms,

$$d_{CF}(X,Y) = d_{ICP}(Z(X), Z(Y)) = \min_{\substack{f:X\to\mathbb{R}^m \\ g:Y\to\mathbb{R}^m}} d_H^{\mathbb{R}^m}(f(X), g(Y)) \tag{8}$$

The term canonical form, computed as Hausdorff distance between the minimum distortion embeddings of two shapes X and Y into some common metric space (Z, d_Z), is used as well. In fact, canonical form is the extrinsic representation of the intrinsic geometry of shape X, and using this, we can transform our nonrigid shape similarity into the rigid similarity problem. Recalling our knowledge of differential geometry, we know that the *Gaussian curvature* is an intrinsic invariant of a surface. As an example, a sphere of radius r has constant Gaussian curvature which is equal to $1/r^2$. At the same time, a plane has zero Gaussian curvature. As a corollary of Gauss's *Theorema Egregium*, a piece of paper cannot be bent onto a sphere without crumpling. Conversely, the surface of a sphere cannot be unfolded onto a flat plane without distorting the distances. Although a truly isometric embedding of shape X is not always possible, we can try to construct an approximate representation of X by minimizing the *distortion* as we defined in equation (1). In our point cloud setting, where the shape X is sampeled at N points $\{x_1, x_2, \ldots, x_N\}$, the distortion criteria will be:

$$\sigma = \max_{i,j=1,\ldots,N} \left| d_{\mathbb{R}^m}(f(x_i), f(x_j)) - d_X(x_i, x_j) \right| \tag{9}$$

The function σ which measures the distortion of distances is called *stress.* As a routine σ_2 is used as the distortion criterion. Considering $Z_i = f(x_i)$ an $N \times m$ matrix of canonical form coordinates and $d_{ij}(Z) = d_{\mathbb{R}^m}(z_i, z_j)$, then:

$$\sigma_2(Z; D_X) = \sum_{i>j} \left| d_{ij}(Z) - d_X(x_i, x_j) \right|^2 \tag{10}$$

Where $D_X = d_X(x_i, x_j)$ is a $N \times N$ matrix of geodesic distances and $d_{ij}(Z)$ is the Euclidean distance between the points on the canonical form. Using this formulation, the coordinates of discrete canonical forms are the solution to the nonlinear least-squares problem:

$$Z^* = \arg\min_{Z \in \mathbb{R}^{N\times m}} \sigma_2(Z) \tag{11}$$

and the minimization algorithms known as *Multidimensional scaling* that are closely related to dimensionality reduction. Elbaz and Kimmel (Elad and Kimmel 2003) used a SMACOF

(Cox 2000) (Scaling by MAjorizing a Complicated Function) algorithm to minimize the stress function.

1.4.4 Geodesic distance interpolation

In practice, the objects are often given as general triangular meshes rather than parametric surfaces and therefore have to be parameterized. In the case of complicated topologies, finding global parameterization is a challenge. The solution is to use local parameterization and a good candidate is to use *Barycentric coordinates*. Each y'_i is represented by a triangle index t_i and a triplet $u_i = (u_i^1, u_i^2, u_i^3)$. Starting with a particular case where y' is one of the mesh vertices: $y' \in y_M$ (Fig. 1.2). In this case, d_1, d_2 and d_3 can be precomputed using the fast marching method. This yields the following interpolation formula:

$$\hat{d}_Y(y, y') = u^1 d_1 + u^2 d_2 + u^3 d_3 = d^T u \tag{12}$$

where $d = (d_1, d_2, d_3)^T$.

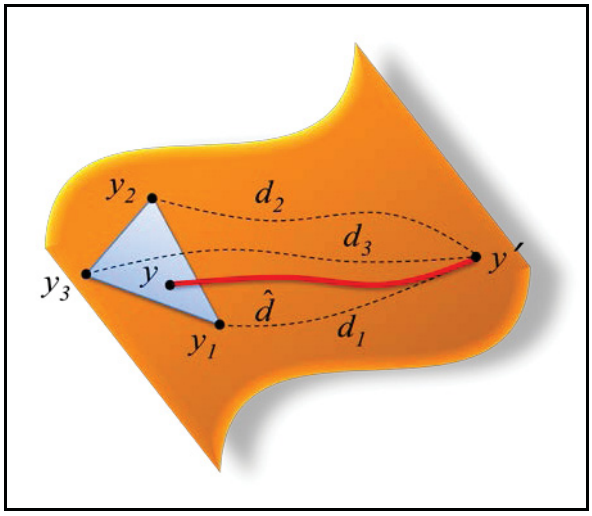

Figure 1.2 Geodesic distance interpolation

If $y' = (t', u')$ is an arbitrary point on the mesh, the distances d_1, d_2 and d_3 are unknown. Once more we assume that y' falls into triangle $t' = (y_4, y_5, y_6)$. Applying the same approach in four steps one can obtain (Bronstein, Bronstein et al. 2007):

$$\hat{d}_Y(y, y') = u'^T D_Y(t, t') u \tag{13}$$

1.4.5 Generalized multidimensional scaling

The main idea is to find the minimum distortion embedding of X into Y which allows quantifying the dissimilarity of the intrinsic geometries of two surfaces. The lowest achievable distance can be demonstrated as embedding distance:

$$d_E(Y,X) = \inf_{f:X\to Y} \operatorname{dis} f \tag{14}$$

We are reminded of the prototype MDS problem with σ_2 stress as equation (10). Here the minimizer is the canonical form of the shape X and the minimum is the embedding distortion σ_2. In practice, the distortion is non-zero, but yet it can be reduced by finding a better embedding space. Replacing the Euclidean geometry of the embedding space with a spherical one usually gives smaller metric distortion (Cox 2000) but still this distortion is not zero. Bronstein et al. (Bronstein, Bronstein et al. 2006) directly embedded X into Y by solving the following problem:

$$\min_{y'_1,\ldots,y'_N\in Y} \sum_{i>j} \left| d_Y(y'_i, y'_j) - d_X(x_i, x_j) \right|^2 \tag{15}$$

We denote the image of x_i in Y as y'_i. The minimum stress value measures how much the metric of X should be distorted in order to fit into Y. Now there is no more need to compare canonical forms and the dissimilarity is obtained directly from the embedding distortion. But the challenge is that, unlike the Euclidean or the spherical cases, there is no more closed-form expression for d_Y (y'_i, y'_j) and metric needs to be approximated, as y'_i are the optimization variables. The computational tool for the interpolation of the geodesic distances on triangular mesh is obtained in previous section. Substituting (13) to the generalized MDS term (15), the quadratic stress function can be obtained:

$$\sigma(t_1,u_1,\ldots,t_N,u_N) = \sum \left(d_X(x_i,x_j) - u_i^T D_Y(t_i,t_j) u_j \right)^2 \tag{16}$$

Generalized stress can be minimized by block coordinate descent algorithms as in (Bronstein, Bronstein et al. 2006) and (Boyd and Vandenberghe 2004). Figure 1.3 tries to construct a simplified representation of similarity measure. The total number of point clouds in two shapes X and Y are represented by n and m, respectively. D_X and D_Y represent symmetric matrixes of pairwise geodesic distances, calculated by fast marching method.

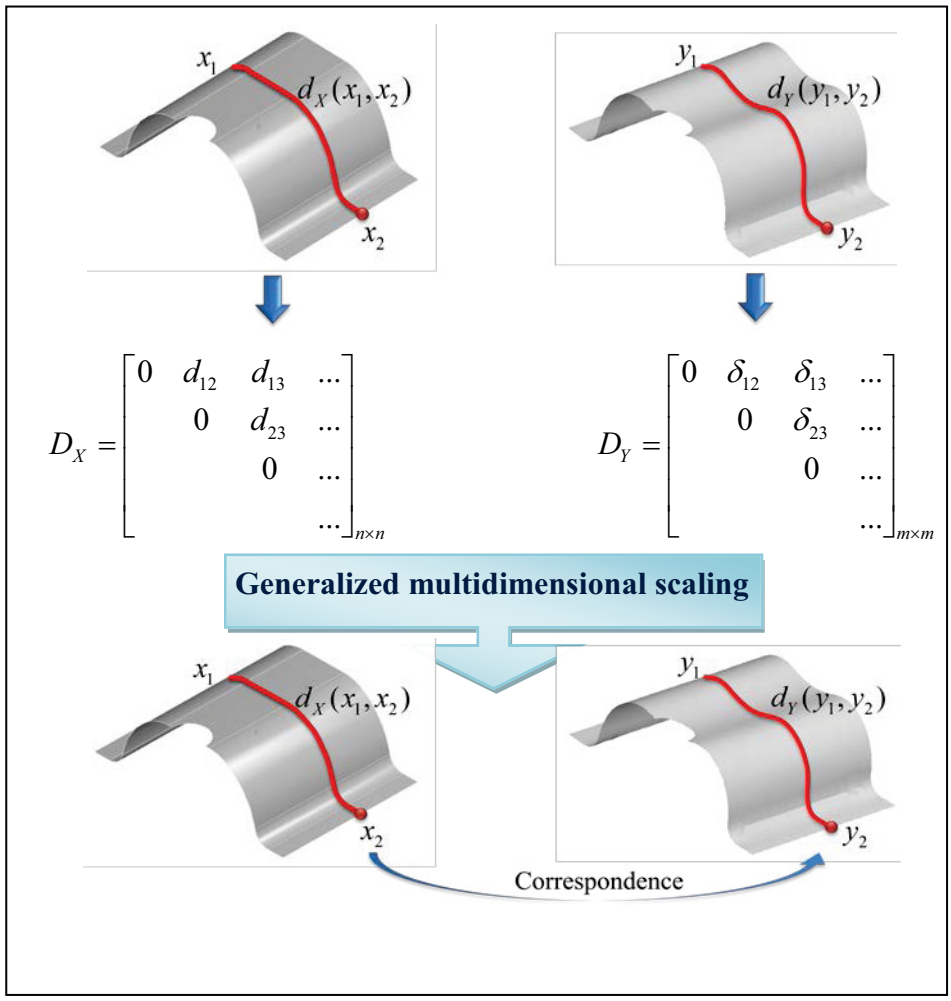

Figure 1.3 Simplified representation of similarity measure

1.5 Nonrigid geometric metrology

Free-state variation is a term used to describe part distortion after the removal of forces applied during manufacture. This distortion is principally due to the part's weight (gravity), flexibility, and the release of internal stresses resulting from fabrication. A part of this kind, for example, a part with a very thin wall in proportion to its diameter, is referred to as a nonrigid part (ASME Y14.5). As the state of weightlessness is rarely possible, the shape of an assembly component is generally defined in the *use state* (constraint state) when joined with other parts. This use state defines the boundary condition, which will define the constrained geometry. When the boundary conditions (or permissible loads) are applied to

the theoretical *free shape*, the geometry of the assembled component is identical to a CAD model and this theoretical free shape can be analyzed with finite element method. The actual free shape is not the same as a theoretical free shape, because it is not possible to elaborate its exact geometry; it includes *geometric deviation*. The free-state does not correspond to the state of weightlessness which we named free shape. In ISO 10579, the position of the part in regard to the direction of the gravity is clearly defined. The condition that occurs when a cold-worked metal part has a tendency to partially return to its original shape is called *spring-back*. This is because of the material's elastic recovery when the forming force is released. This severely affects the dimensional accuracy of the part. The proposed inspection method should be effectively capable to explain the material behavior during registration between free-state (scanned point cloud) and nominal CAD data. At this stage, assuming the availability of scanned point clouds, the goal is to register two clouds of points, the first belongs to a CAD model and the second belongs to range data obtained in free-state. For flexible parts and before scanning, one should take into consideration the effect of spatial positioning (part set-up) in the final geometrical form of scanned data. Without knowing the important fact of gravity direction, serious errors in results can be predicted. Thus, before scanning, the part is setup onto reference support points in which their position is clearly defined within the part frame. Note that the set-up must not be over-constrained, unless otherwise specified according to designer request (ISO 10579). In this case, the same constraints must be taken into consideration during finite element analysis.

1.5.1 Identification of geometric deviation

Let x_i be the theoretical point obtained within a CAD model, and x'_i its correspondence obtained from finite element analysis and finally y'_i the correspondence of two premier points in range data. Assuming linearity, for geometrical deviation, the following equation can be derived:

$$[R_{real}] = [R_{measured}] - [R_{theorical}] \tag{17}$$

which $[R_{measured}] = x_i\, y'_i$ is the geometrical deviation between point clouds of CAD model and the measured surface. $[R_{theorical}] = x_i\, x'_i$ results from the finite element simulation of the part in free-shape state, in addition to gravity. As mentioned before, the same set-up

constraints applied to the scanning process must be taken into consideration as boundary conditions. At this stage, real geometrical deviation [R_{real}] can be calculated. Correspondence between x_i and x'_i is evident; the challenge is how to find the y'_j which corresponds to x_i.

Let X and Y be metric spaces with metrics d_X and d_Y; the first correspond to the CAD model and the second to scanned range data. Due to the fact that x_i and y_i belong to two different metric spaces; similarity measure cannot be computed using Hausdorff distance. Assuming that our deformation is a distance preserving one, that is to say $d_X(x_i, x_j) = d_Y(y'_i, y'_j)$. Thus, our goal is to find a mapping like $f: X \rightarrow Y$, by solving the problem (15) where the y'_i is the image of x_i in Y. The minimum stress value measures how much the metric of X should be distorted in order to fit into Y. To this end, GMDS can be used to find the correspondence between simulated CAD and scanned clouds of points. Mathematically speaking, the embedding process does not need primary surface registration (X and Y are different metric spaces). In the next section we propose a *generalized numerical inspection fixture* which is a new challenge for getting rid of conventional inspection fixtures.

1.5.2 Generalized numerical inspection fixture (GNIF)

The part is setup onto reference support points where the position is clearly defined within the part frame. These points, as priori information, will be utilized as the boundary condition, where it will simulate the gravity and support effect on the CAD-model. The part is scanned in a distorted state without a fixation device. Preprocessed measured data is put together with the CAD-model. Note that the CAD-model should be previously analyzed, applying the gravity and support effects in the same direction as the scanning process (Fig. 1.4). The transformations that map the preprocessed CAD-model towards range data can be obtained by a regular ICP method. In practice and at this stage, we put the measuring part on the inspection fixture. In our methodology, this range data plays the role of inspection fixture and we call it numerical inspection fixture. Again we notice that mapping the CAD-model into range data has some advantages. Transforming the range data into a computer-aided analyzable model especially for complicated surfaces is a very time consuming process. For such surfaces, more human intervention is needed. Furthermore, parts with hidden stiffening

structure or other details at the back side of scanned surface, are so difficult to be modelized as FEM-analyzable model. The main advantage of proposed method is that only one FEM-analyzable model should be created. This really decreases inspection time specially is mass production. Using geodesic distance as a similarity measure tool, enable us to find the correspondence between CAD-model and range data even in the presence of large deformations. Also note that embedding process does not need primary surface registration, so the similarity detection can take place before the rigid registration. If we suppose that there is no a priori information for the assembly process, then the contour or other assured points with negligible deformations such as rigid attachments can be used for nonrigid mapping of preprocessed CAD-model into the range data. Generalized multidimensional scaling can be used as isometry-invariant partial surface matching so there is no need for perfect contour hypothesis. This is very useful when dealing with parts containing missing data. Defects due to geometric deviation can be found after *finite element nonrigid registration*, eliminating the spring-back effect. Also note that the meshed CAD-model and the scanned workpiece may have a different number of vertices (as in Figure 1.5).

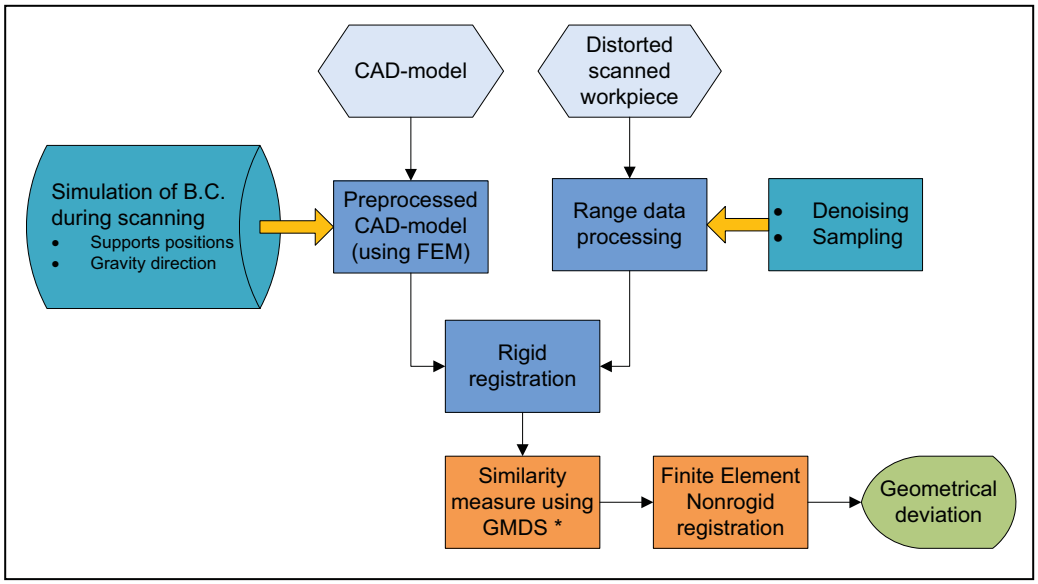

Figure 1.4 Inspection process flowchart using GNIF

*Similarity measure can also be done before rigid registration.

The part can be scanned in a production line or it is indispensable to the fast scanning process. The other steps are realized offline using a PC, thus there is no more need to stop production lines for testing a part.

1.6 Results

We have tested presented methodology in a series of typical mechanical parts. This section presents four case studies containing free-forms, sharp edges and discontinuities (holes) and with different sizes that evaluates performance and validates the methods developed in previous sections. To this end, the free-form model is simulated by CATIA® and ANSYS® then a finite element analysis of the model is done simulating the free-state range data. At this step, an external force is applied to the model to simulate unknown spring back deformation. Predefined profile defect was also added to all case studies. Due to the fact that we have used predefined deformation in range data generation steps (spring back and profile defect), qualitative performance evaluation is effectively traceable. Point clouds of free-form and free-state are simulated with a different number of vertices to evaluate the geodesic distance interpolation. We have used *Voronoi tessellation* in order to represent the sampled discrete nodes of (metric) surface. After ICP based rigid registration, similarity detection has been done using GMDS. Then CAD-model was mapped towards range data using detected points. Still in the absence of prior information about assembly process, contour points along with holes can be used using correspondent points. We used the contour points for nonrigid registrations. Only the maximum geometric deviation is presented (Table 1.2). For better visualization, a sampled tessellated section of the third case study with 100 sampled points is illustrated in Figure 5. Geodesic distance interpolation enables us to accurately measure the similarity between the CAD and scanned data; still there is no exact nodal correspondence. In rigid registration process, some prior defined points, or in the areas with the least defect probability, may be used for increasing the procedure speed. Overall size and engineering properties of the four case studies are represented in Table 1.1. The results are shown in Table 1.2.

Table 1-1 Overall size and engineering data

1st case study	2nd case study
 1400x1000x450 t=0.5	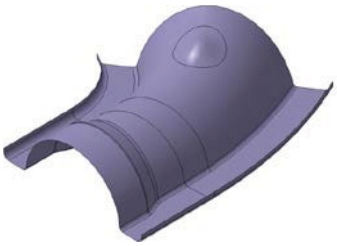 80x60x23 t=0.5
3rd case study	**4th case study**
 330x130x78 t=0.2	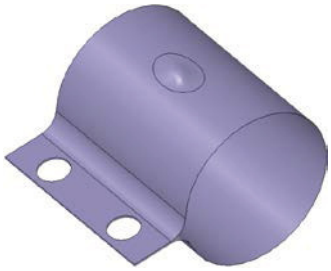 ϕ80x100 t=0.5

Note: Profile defect area is presented by a circle.
Dimensions are in *mm*.
Young's modulus = 2e+11 Pa
Poisson's ratio = 0.3

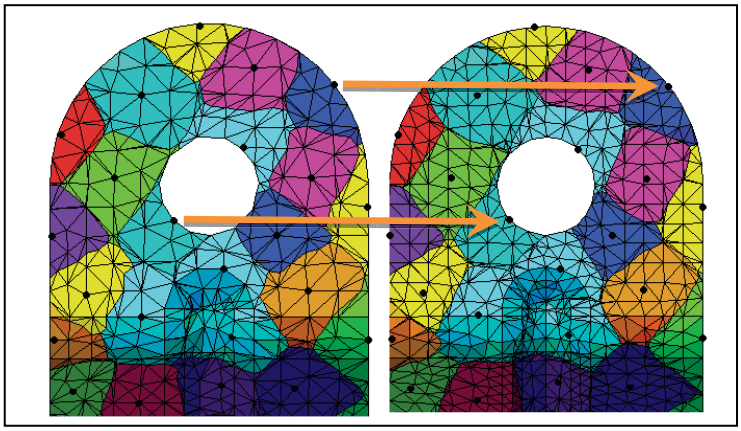

Figure 1.5 Similarity measure between CAD-model and range data, for the 3rd case study (Enlarged view of upper section. Bold black points represent the sampling by Voronoi tessellation.)

Table 1-2 GNIF verification

	1st case study R_{max} [*mm*] #	*2nd case study* R_{max} [*mm*]	*3rd case study* R_{max} [*mm*]	*4th case study* R_{max} [*mm*]
GNIF Results	5.34 (200)*	0.79 (100)	0.86 (100)	0.55 (200)
	8.74 (500)	1.01 (200)	1.20 (300)	1.10 (500)
	9.93 (1000)	1.10 (500)	1.73 (500)	1.44 (1000)
Maximum predefined profile deviation+	10	1. 5	2	2

* The values between parentheses represent sampled points on CAD-model and range data.
# Maximum geometric deviation calculated by GNIF.
+ Considered as reference value.

All case studies were performed on an AMD Phenom(tm) II X4 B95 Processor 3.00 GHz PC using a 64-bit operating system. For instance, similarity measure on first case study and for 200, 500 and 1000 sampled points took 1.5min, 9.7min and 37.5min, respectively. Correspondence search and putting the results with nonrigid registration algorithm are the main computational demanding steps. As expected, increasing the density of sampled points causes more accurate results (see case studies by column in Table 1.2). On one hand, in order

to better represent the underlying surface deviation, we prefer the point sampling to be as densely as possible. On the other hand, we need to keep in mind that the discrete representation is used by computer algorithms, and every additional point increases storage and computational complexity costs.

When acquiring three-dimensional shapes using range cameras, a phenomenon called *topological noise* is a well-known problem. Topological noise affects the intrinsic geometry of shape. In order to evaluate the effect and robustness of the presented methodology we contaminated the range data of the third case study by Gaussian noise of mean $\mu = 0$ and standard deviation $\sigma = 0.03$ *mm* which is independently distributed in each node. Choosing the Gaussian noise was because of their simplicity for simulation. Although some researches (Sun, Rosin et al. 2008) demonstrate that real scanner noise is neither Gaussian, nor independently distributed. With different iterations we have found up to 0.14 *mm* deviation, passed from what was calculated at noiseless case with 500 sampled points. This means that topological noise strongly affects the intrinsic geometry of surface and similarity measure. Topological noise may have serious consequences if it affects the connectivity of nodes. Connectivity changes definitely touch the geodesics. Consequently, if we try to compute the canonical forms, they will absolutely have different forms. For the fourth case study, in arrowed point, topological noises affect the canonical form as illustrated in Figure 1.6.

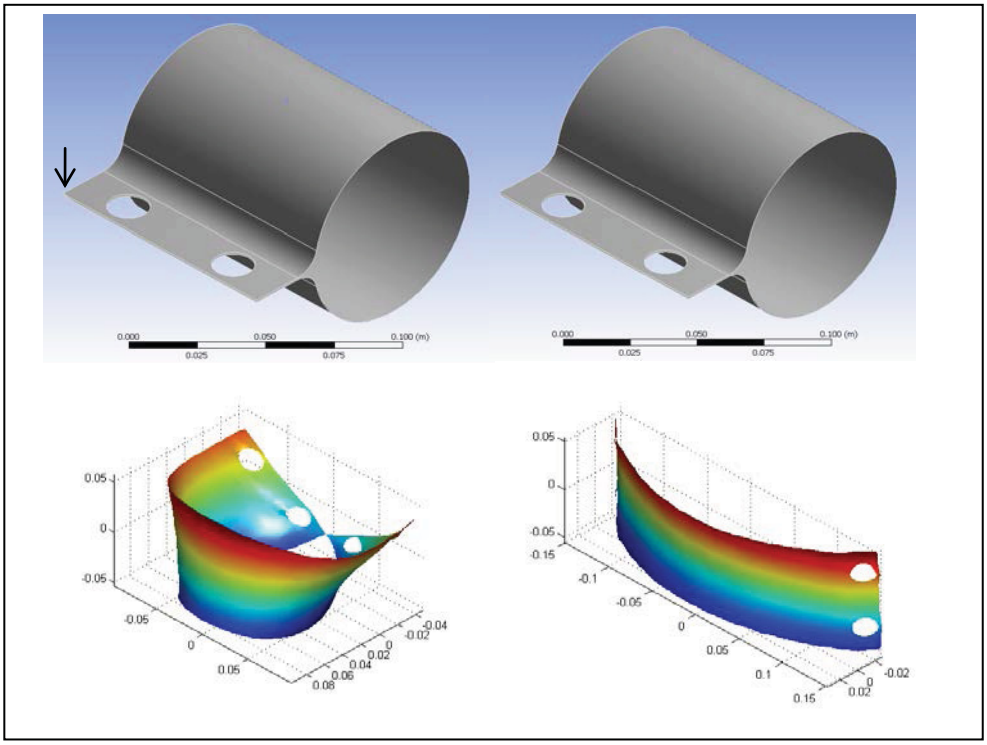

Figure 1.6 Effect of the topological noise on the computation of canonical forms.

1.7 Conclusion

Including *part compliance* with *intrinsic geometry* of surfaces in the metrology of free-form surfaces is an area of research pioneered in this study. We merged the technologies in metric and computational geometry along with statistics and finite element methods to develop a general approach to the geometrical inspection of nonrigid parts. This method enables us to verify a diverse range of flexible parts without using special inspection fixtures. Although we have tried to present convincing results, no method with such promise is likely to be widely accepted until more practical testing can be done. Despite the fact that the proposed GNIF method is quite efficient, there is plenty of work to do for future computational speedup and accuracy. As a matter of fact, the proposed method is not a perfect and faultless substitution for inspection fixtures and CMM reports. However, in real-time applications it can be used for variational control of production lines so there will be no more need to stop production to test a workpiece.

In the proposed inspection methodology, and for a full process automatization, we used the contour for nonrigid, isometry-invariant surface matching. In fact, this is the only way to proceed when there is no prior knowledge of assembly joints and areas. This is not what to expect for a vast range of engineering applications. For more crucial results, prior information in assembly joints is needed. In production lines, and for each series of products, this information is available, so full automatization of the inspection process is still possible. Unlike the methods presented by other authors to find the similarity between a CAD-model and range data (two different metric spaces), presented embedding processes do not need primary surface registration. This really speeds up the measuring process, especially given prior information about the assembly process. One of the significant specifications of GNIF was the capability for isometry-invariant partial surface matching. This means that contour matching can be safely utilized in the existence of missing data. Proposed similarity measure is suitable for large deformations. Correspondence search is also completely automatic.

We did not deal with the effect of the diverse smoothing methods to reduce the topological noise effect. Also, uncertainty associated with the material properties has not been considered. These methods as well as the effect of material uncertainty should also be studied in depth. With modern technologies in laser scanners, millions of points presenting the topology of surface are accessible. This means that the sample Dijkstra algorithm in graphs may give the closest results in comparison with the fast marching method. This is something that requires further experiments. Actually, this study may be criticized due to a lack of practical experiments. In spite of the fact that we tried to present persuasive results, there is no equivalent method for comparison and accurate assessment. Future work should expand and verify our presented methods with practical tests. Presently we are developing a more accurate geodesic distance calculation in discrete domains. Further deepening of this research would involve studying measuring uncertainty and classifying it with surface extrinsic geometry.

CHAPITRE 2

ROBUST GENERALIZED NUMERICAL INSPECTION FIXTURE FOR THE METROLOGY OF COMPLIANT MECHANICAL PARTS

Hassan RADVAR-ESFAHLAN; Souheil-Antoine TAHAN

Laboratoire d'ingénierie des produits, procédés et systèmes (LIPPS)

École de technologie supérieure

Montreal, Canada, H3C 1K3

Article published on-line in « *International Journal of Advanced Manufacturing Technology* », (September 2013)

2.1 Abstract

Free-form non-rigid parts form the essence of today's automotive and aerospace industries. These parts have different shapes in *free state* due to their dimensional and geometric variations, gravity and residual strains. For the geometric inspection of such compliant parts, *special inspection fixtures* are used in combination with coordinate measuring systems (CMM) and/or optical data acquisition devices (scanners). In our previous work, a general procedure was developed to eliminate the use of inspection fixtures. We measured the similarities between CAD model and scanned data by taking the advantage of the geodesic distance metric. Then, using finite element non-rigid registration, we deformed the CAD model into range data to find the geometric deviations. Here, we apply a new method to robustify the *generalized numerical inspection fixture* (GNIF). We filter out points causing incoherent geodesic distances, and demonstrate that our approach has several significant advantages, one being the ability to handle parts with missing range data. The other advantage of the method presented is its capacity to inspect parts with large deformations.

Keywords: Geometric inspection, Compliant part, Intrinsic geometry, Geodesic distance, Finite element non-rigid registration, Multidimensional scaling

2.2 Introduction

Geometric inspection, geometric modeling, range data acquisition and analysis have developed as separate fields of engineering among different engineering and scientific communities. However, all these fields share a common scientific concept, and the opportunity cost for the lack of their mutual connections is a waste of the synergy which could otherwise exist. Computer-aided inspection is one of these connection points, while non-rigid geometric inspection shares a profound degree of understanding of all the mentioned disciplines. Currently, a flexible workpiece must be fixed or clamped during the measurement process in order to simulate the *use state*. To that end, special inspection fixtures need to be designed and manufactured. On the other hand, some inspection stages cannot be fully automated with this conventional approach. As a result, the geometric inspection of flexible parts remains a time- and money-consuming process. For example, according to our industrial partner (Bombardier Aerospace), some inspection *set-up processes* for non-rigid parts demand 60 to 75 hours of operations. On the other hand, even for simple parts, the quality of a planned inspection depends on the ability and experience of the operator. Despite the tons of papers and research that have been produced in the CAD, CAM and CAI (computer-aided inspection) fields, the inspection of flexible parts continues to pose difficulties and to impose significant cost on industries because they need special fixation devices. This also points to a lack of knowledge and theoretical foundations surrounding this special field. Our approach (Radvar-Esfahlan and Tahan 2011) represents an effort to eliminate the use of special inspection fixtures in the metrology of flexible parts. However, the method has some drawbacks, which we present here in greater detail, with respect to the algorithms used. The other aim of this paper is to robustify the algorithm mentioned. Before getting into the details of the proposed inspection methodology, we begin by defining some of the terms used in this paper.

Definition 1. A "*Non-rigid part* is "a part which deforms to an extent that in the free-state is beyond the dimensional and/or geometrical tolerances on the drawing." [ISO 10579:2010]
Definition 2. "*Free-state* is the condition of a part subjected only to the force of gravity." [ISO 10579:2010]
Definition 3. "*Free-state variation* is the distortion of a part after removal of forces applied during manufacture. This distortion is principally due to weight and flexibility of the part and the release of internal stress resulting from fabrication. A part of this kind (e.g. a part with a very thin wall in proportion to its diameter) is referred to as a *non-rigid part*." [para. 5.5 ASME Y14.5-2009].
Definition 4. *Isometric deformation* is a kind of deformation in which the geodesic distance between points is preserved during deformation.
Definition 5. *Isometric embedding* is a distance preserving mapping.

The remainder of this paper is structured as follows. Section 2 provides a comprehensive literature review on rigid and non-rigid registration methods, range data segmentation and the metrology of flexible parts. In Section 3 the robust version of GNIF will be introduced in details. To this end, this section is divided into five sub-sections. Brief discussion on fast marching method will be introduced in Section 3.1. Section 3.2 gives an introduction on isometric embedding as a measure used in this paper for similarity detection. As the main contribution of this paper is the improvement of GNIF, *incoherent geodesics* will be introduced in Section 3.3. Finite element non-rigid registration (FENR) and geometric inspection process of flexible parts will be discussed in Sections 3.4 and 3.5, respectively. Section 4 gives verification and validation of presented methodology using four case studies. Finally Section 5 presents conclusions.

2.3 Prior works

2.3.1 Rigid and non-rigid registration

Simultaneously with mechanical engineers, but in different fields, such as Computer Vision, Biomedical Engineering and Pattern Recognition, the engineers have conducted a great deal of research on rigid and non-rigid registration and deformable surface comparison. Besl and McKay (Besl and McKay 1992) developed the *Iterative closest point* (ICP) algorithm, an iterative method for the rigid registration of 3D shapes, and one of the common techniques for 3D rigid surface registration. With two shapes on hand, X and Y, the goal of ICP is to find the rigid transformation which would bring the two as close as possible. The closeness is measured by the *Hausdorff distance* between two shapes. Many versions of ICP have been proposed. These methods differ from the selection and matching of points, to the minimization strategy (Bentley 1975, Greenspan and Godin 2001). We refer the reader to (Rusinkiewicz and Levoy 2001) for an account of, and comparison between, some ICP variants. In (Holden 2008), Holden provides a comprehensive and quantitative review of spatial transformation models for non-rigid image registration.

Multidimensional scaling (MDS) (Borg and Groenen 2005), which is widely used and developed in human sciences like sociology and economy, used to serve as a bridge to represent the intrinsic geometries of the shapes in a common metric space where they could be compared using rigid similarity algorithms. In (Schwartz, Shaw et al. 1989), the authors flattened the convoluted surfaces of human brains in order to carry out mutual comparisons, and finally, to study the functional architectures of the brain. Some people consider their work to have been a breakthrough in which surface geometry was translated into a plane. Starting from the first generation of MDS until now, many variants of minimization algorithms have been developed for minimizing the stress function. One of the most straightforward and successful among these was developed by de Leeuw (De Leeuw 2005). In (Elad and Kimmel 2003), the authors presented the concept of *Invariant Signature* for surfaces. Their method used *fast marching* on triangulated domains, followed by the MDS technique. They transformed the problem of isometric-non-rigid surface matching into a

matching of rigid surfaces problem. Using MDS, they embedded surfaces *X* and *Y* into a common embedding space *Z* called a *Canonical form*, and then measured their similarity using the *Hausdorff distance*. Their method is strongly based on the Kimmel and Sethian (Kimmel and Sethian 1998) method in computing the geodesic distance on triangular meshes. As the nature of their study was based on classification and pattern recognition, the accuracy of their presented method as a measure of the similarity of metric spaces was not discussed. On the other hand, the uncertainty of canonical forms due to geodesics based on the fast marching method, as well as the uncertainty related to the least square multidimensional scaling process, should be investigated in depth. Because the similarity measure plays a critical role in our special case, the accuracy of canonical forms in cases of non-rigid inspection will be studied using real engineering case studies.

Despite of canonical forms in which two metric spaces were mapped into a common space, Bronstein *et al.* (Bronstein, Bronstein et al. 2006) proposed a method which mapped two metric shapes directly into one another. In spite of classic MDS, here the distortion was a kind of similarity measure tool. The distortion showed the degree to which two shapes are similar (or dissimilar). Another advantage of their method is its ability to measure the similarity of shapes in which no exact nodal correspondence exists between the sets of range data. The presented method was also suitable in cases of partial matching.

2.3.2 Point cloud segmentation

In spite of world's continuous phenomena, usually in engineering applications such as image processing and computer vision, we encounter issues with discrete data. In our application (i.e. geometric inspection), features of range data captured by optic scanners should be extracted. To this end, the edges play an important role as one of the feature detection tools. Various approaches have been proposed for detecting edge points in measured range data. Chen and Schmitt (Chen and Schmitt 1992) presented a method for calculating principal curvatures on a triangulated surface. Yang and Lee (Yang and Lee 1999) used surface curvature properties to detect edge points. They investigated the behaviour of the surface curvature in a cross-section of the surfaces: step edge, crease edge, edge formed by a

concave/convex surface and a flat surface, and finally, an edge formed by a concave and convex surface. If the range images are relatively noise-free, then the first the two principal curvatures can first be computed followed by the zero crossing and extrema of the largest principal curvature.

Alrashdan *et al.* (Alrashdan, Motavalli et al. 2000) proposed a hybrid segmentation approach, involving the edge-based segmentation performed by the Kohenon network to detect step and roof edge points. They used Laplacian filter and surface normal values at each point as an input of the Kohenon network; after which they then used mean and Gaussian curvatures in order to perform the region-based segmentation. The next step was the integration of the two previous steps.

In (Anguelov, Taskar et al. 2005, Munoz, Vandapel et al. 2008), and more recently (Shapovalov and Velizhev), the authors address the problem of object class segmentation of 3D range data using Markov random fields. Although MRF-based methods give acceptable results in object recognition, for feature detection (i.e., finding the boundaries, sharp edges and corners which are the subject of similarity measuring process), this method should be combined with others. On the other hand, the accuracy of MRF-based methods in the correspondence measure of the metric space should be investigated in depth. In this paper, as one of the essential steps of our methodology, a novel method of contour detection will be presented.

2.3.3 Geometric metrology of non-rigid parts

3D geometric inspection of free forms has become an integral part of automotive and aerospace industries. Despite the revolution that has occurred in computer sciences and digital data acquisition devices such as laser scanners, non-rigid shape measurement is strongly based on using fixation devices to simulate the state of use. Free-form, non-rigid geometrical inspection has not undergone extensive study, and state-of-the-art industries still use fixation devices for this purpose. A state-of-the-art review of the most important measuring techniques is presented in (Chen, Brown et al. 2000, Savio, De Chiffre et al. 2007), along with their capacity for free-form measuring tasks. For all these methods

presented (Li and Gu 2004, Li and Gu 2005, Gao, Gindy et al. 2006, Shi and Xi 2008), the manufactured part is assumed to have a similar shape as the CAD model, allowing for comparison. Li *et al.* (Li and Gu 2005) used a two-step registration, and employed some local surface properties (e.g., Principal and Gaussian curvature) in order to find the coarse correspondence between CAD model and range data. They then performed fine localization based on the least square principal. The benefits of their method in comparison to the single-step ICP algorithm are not discussed. All presented methods, and most recently Ravishankar *et al.* (Ravishankar, Dutt et al. 2010), use rigid registration as a similarity measure.

Early efforts at non-rigid inspection were undertaken by Weckenmann and Gabbia (Weckenmann and Gabbia 2005), who proposed a measuring method using virtual distortion compensation. The idea behind their method was to deform the actual distorted point cloud into the nominal use state (CAD model). Feature (e.g., holes and edges) extraction was the key to measuring the correspondence between CAD model and range data. From the acquired point cloud, a triangle mesh of the surface was generated, and then the meshed surface was transformed into an FEM model to simulate the fixation process by using extracted features as the boundary condition. Their method was not completely automated because the suggested method posed some human challenges in terms of identifying the correlation between some special points like holes and assembly joint positions. These were used by the controller to find the boundary conditions of the FEM problem. Furthermore, transforming the point cloud to a computer-aided analyzable model is a very time consuming process. These drawbacks were then largely tackled in (Weckenmann, Weickmann et al. 2007). To that end, they deformed the CAD model and mapped it towards range data, thus decreasing the time of inspection. An FEM mesh created from a CAD model also provided more precise results than a triangle mesh from measurement results. However, the proposed method still required human intervention in order to find the correspondence between CAD model and range data.

The *Small Displacement Torsor* (SDT) concept was developed by Bourdet and Clément (Bourdet and Clément 1976) to solve the general problem of a geometrical surface model fitted to a set of points using rigid body movements. Lartigue *et al.* (Lartigue, Theibaut et al. 2006) took advantage of the possibilities offered by voxel representation and the SDT

method for the dimensional metrology of flexible parts. They considered the effect of gravity and the spatial location of a scanned part. This method is fundamentally based on finding the correspondence between the cloud of all measured points and CAD meshed data. In fact, the SDT is not suitable in the presence of large deformations.

Abenhaim *et al.* (Abenhaim, Tahan et al. 2011) developed an *Iterative Displacement Inspection* (IDI) which smoothly deformed the CAD mesh data until it matched the range data. Their method was based on optimal step non-rigid ICP algorithms (Amberg, Romdhani et al. 2007). The point cloud had to be dense enough because the method's similarity measure was based on the nearest distance calculation. The method depended on finding some flexibility parameters which could vary according to thickness. They used the same number of nodes in two datasets, which rarely happens in real applications.

Radvar-Esfahlan and Tahan (Radvar-Esfahlan and Tahan 2011) merged the technologies in metric and computational geometry with statistics and finite element methods to develop a general approach to the geometrical inspection of non-rigid parts. By taking the advantage offered by the geodesic distance metric, they measured the similarities between CAD model and range data. Then, using finite element non-rigid registration (FENR), they deformed the CAD model into range data to find the geometric deviations.

Recently, in (Jaramillo, Prieto et al. 2013, Jaramillo, Prieto et al. 2013) the authors proposed a methodology that used the partial range captures of the workpiece. The inspection process was based on an iterative nonrigid alignment algorithm. To this end, a transformation to the CAD model was applied at each iteration which was calculated by minimizing the error with a partial-view model. By this method it was assumed that the acquired region contains sufficient feature points that would enable model alignment. We underline that the ability of partial inspection is one of the capabilities of the GNIF technique first presented in (Radvar-Esfahlan and Tahan 2011).

While previously mentioned methods seek a quantitative analysis of nonrigid parts (geometric deviation), qualitative visual inspection of these parts using light-reflection patterns were first introduced by Gentilini and Shimada (Gentilini and Shimada 2011). Although the accuracy of their method was acceptable (0.3-0.6mm) for average industrial

applications, those kinds of defects are widely traceable with machine/computer vision technologies.

2.4 Robust numerical inspection fixture (RNIF)

In (Radvar-Esfahlan and Tahan 2011), we presented a methodology based on the fact that the shortest inter-point path (geodesic distance) between any two points on the parts remains unchanged during an isometric deformation. We called this property a *distance preserving property of non-rigid parts*. Here, we provide a more detailed image of the property. The aim is to construct a more robust algorithm. To this end, we will filter out some geodesic distances which influence our algorithm. Using depicted examples, we will discuss the source of such incoherent geodesics.

2.4.1 Geodesics on range data

Fig. 2.1 shows a thin-wall part deformed under its weight. Let x_i be the theoretical point within a CAD model and let y_i' represent the image of x_i in Y on free state; where $x_1,...,x_n \in X$; $y_1',...,y_m' \in Y$ and n, m are the sampled points which represent two spaces X and Y. Despite the large deformation present, the two shapes are *intrinsically similar*, which means that it is possible to unfold one surface onto the other without stretching it (in the absence of plastic deformations), i.e., a map of one surface can be unfolded over the other, while preserving its distance. The shortest path (geodesic distance) between x_1 and x_2 remain unchanged during isometric deformation, so $d_{x_1x_2} = d_{y_1'y_2'}$. As we will discuss later, this property enables us to find the correspondence between CAD model and scanned data. Mathematically speaking, intrinsic properties remain unchangeable due to isometric deformations, and so to compare the non-rigid shapes, we should look at their intrinsic geometries. In other words, since X and Y belong to different metric spaces $\mathbb{R}^3$, we cannot measure their similarity using a *Hausdorff distance*-based similarity measure (e.g., ICP).

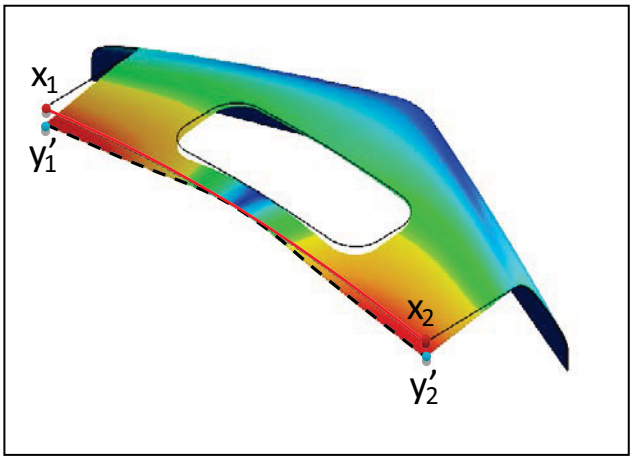

Figure 2.1 Intrinsic similarity in deformed shapes

The first and most important step of our approach is therefore to approximate the pair-wise geodesic distance between all points on range data and CAD model. If the sampling domain is dense enough, one idea is to approximate the geodesic distance between points with the famous *Dijkstra shortest path algorithm* (Dijkstra 1959); however, the shortest path computed by the Dijkstra algorithm does not always yield the real shortest path. For example, we may consider a unit square graph and its shortest path between the upper left and lower right angles, which is equal to $\sqrt{2}$ while the shortest path calculated by the Dijkstra algorithm is equal to 2. This problem is due to the fact that we are allowed to move in the graph using only nodal points. To overcome this inconsistency of the Dijkstra algorithm, the *Fast Marching Method* (FMM) was introduced by Sethian (Sethian 1996) as a numerical method for solving boundary value problems of the *Eikonal* equation:

$$\left|\nabla T(x)\right| F(x) = 1, \qquad T(X_0) = 0 \tag{18}$$

which describes the propagation of a closed curve in $\mathbb{R}^2$ (or a surface in $\mathbb{R}^3$) with speed F in the direction normal to itself so that the sign of the speed function never changes. Kimmel and Sethian (Kimmel and Sethian 1998) developed a version of the Fast Marching algorithm on triangulated domains with the same computational complexity. The initialization of T was, like in Dijkstra algorithm, zero at X_0. Unlike the Dijkstra algorithm, where the shortest path was restricted to graph vertices, the shortest path in the FMM can pass through the triangular mesh. Fig. 2.2 (left) depicts the idea behind the FMM in the triangulated domain. Let us assume that we are given two points x_1 , x_2 with known front arrival times T_1 and T_2. The

question is how to estimate the front time T_3 when it arrives at the point x_3. Note that we can freely switch between the path length and arrival time, thus d_1=T_1, etc. In this case, d can be calculated as the point-plane distance $d_1 = n.x_1+p$, $d_2 = n.x_2+p$. These two equations can be written with matrix notation as follows:

$$V^T n + p.1 = d \tag{19}$$

where $d = [d_1, d_2]^T$, $V = [x_1, x_2]$, $1 = [1, 1]^T$. The unit normal vector n can be easily drived from equation (2).

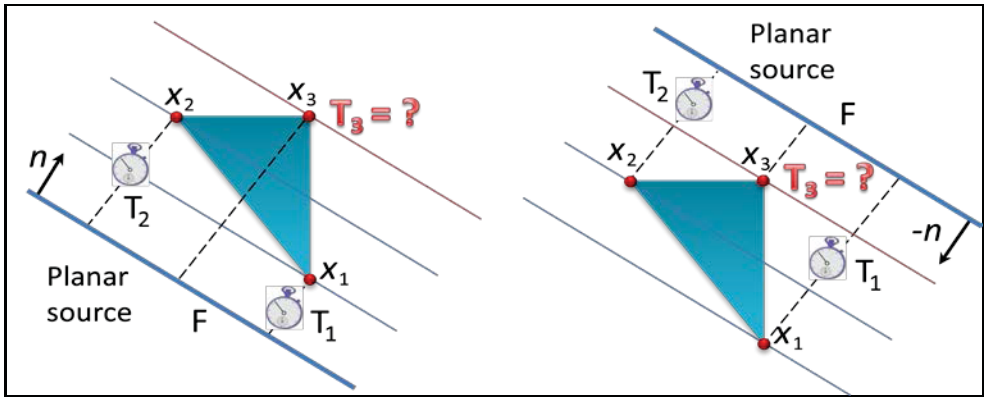

Figure 2.2 Calculation of arrival time in $\mathbb{R}^2$ for an expanding front F>0

Assuming that the front is planar ($x_1, x_2, x_3 \in \mathbb{R}^2$), the discretization of the Eikonal equation leads to the following quadratic equation (Bronstein, Bronstein et al. 2007):

$$d_3^2.1^T Q1 - 2d_3.1^T Qd + d^T Qd - 1 = 0 \tag{20}$$

where $Q = (V^T V)^{-1}$. Equation (20) has two solutions, with both n, $-n$ satisfying it. In this case, the smaller solution is not acceptable (Fig. 2.2, right) because the front propagation time is a monotonically increasing function, which means that $d_3 > d_1, d_2$. This is equivalent to saying that $V^T n < 0$.

Another effect of this monotonicity can be translated as:

$$\left(\frac{\partial d_3}{\partial d_1}, \frac{\partial d_3}{\partial d_2} \right)^T > 0 \tag{21}$$

which means that d_3 should increase when d_1, d_2 increase or simply $QV^T n < 0$. Given that $Q = (V^T V)^{-1}$ then $QV^T V = (V^T V)^{-1} V^T V = I$. This means that the rows of QV^T are orthogonal to

triangle edges, which mean that n must lie within the triangle and $\angle x_1x_3x_2$ should be acute. Thus, the entire update step can be summarized as in Algorithm 1.

Algorithm 1 Fast marching update

input: triangulated surface
output: shortest inter-point path

1 Solve the quadratic equation (3) and select the larger solution.
2 Compute the front propagation direction n.
3 **if** $QV^T n > 0$
use Dijkstra's algorithm:
$d_3 = \min\left\{d_1 + \|x_1 - x_3\|_2, d_2 + \|x_2 - x_3\|_2\right\}$
else
$d_3 = \min\{d_3, p\}$

In the case of obtuse meshes in (Kimmel and Sethian 1998), the authors propose to split the obtuse triangle into two acute ones.

2.4.2 Isometric embedding

Fig. 2.3 depicts two similar non-rigid shapes. As stated in the previous section, our goal is to compare and find the correspondence between shapes X and Y with the metrics of d_X and d_Y. In most non-rigid part applications, the deformations are isometric. This means that two shapes X and Y, in spite of deformations, are isometrically equal. In this case, because the two metrics are different, we cannot find their similarity using Hausdorff-based methods like ICP.

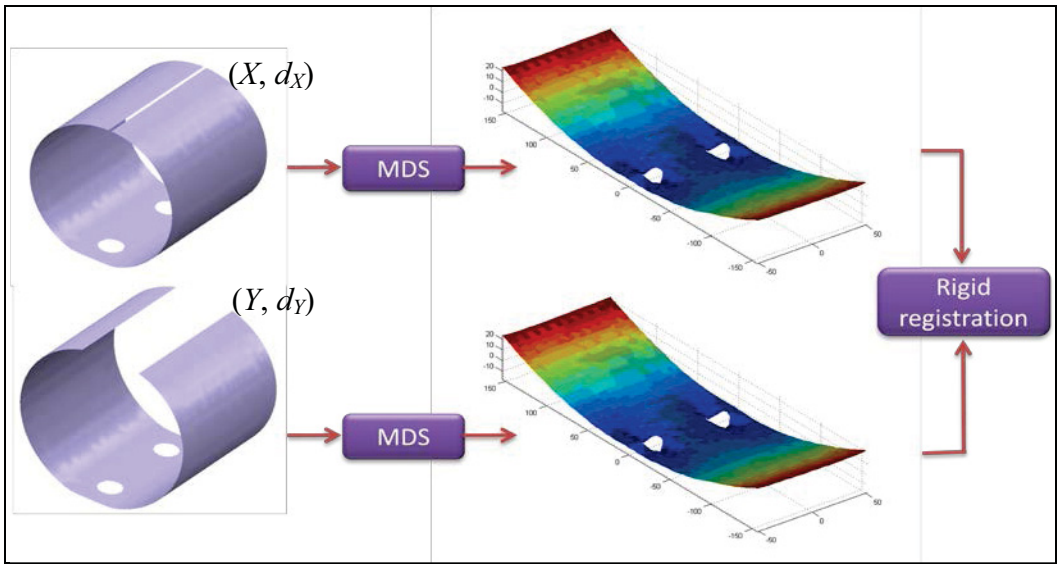

Figure 2.3 Illustration of the isometric embedding problem

In fact, non-rigid registration is somewhat difficult than the rigid registration. Despite the rigid case, here we should be looking for the intrinsic similarity because intrinsic geometry remains unchanged during isometric deformations. Fig. 2.3 also demonstrates a method for dealing with the non-rigid registration problem. Let us assume that we are capable of embedding two shapes (left) in a common metric space (right). If we can construct this embedding such that the Euclidean distance between all inter-point nodes during embedding remain equal in terms of geodesics, in this case we can transform a non-rigid similarity problem into a rigid registration problem. This method seems like an ideal method for the non-rigid registration problem. The problem now is how to map the shapes onto a common space in an ideally isometric manner. From geometry we know, for example, that mapping a sphere onto a flat surface (and vice versa) produces unwanted distortions, because both the sphere and the flat surface have different Gaussian curvatures. One way of overcoming such a problem is by trying to construct an approximate construction by minimizing the distortion. This is the basic idea behind the *canonical forms* proposed in (Elad and Kimmel 2003). In our point cloud setting, where the shape X is sampled at N points $\{x_1,x_2,\ldots,x_N\}$, the *distortion* (Burago, Burago et al. 2001) criteria will be:

$$\sigma = \max_{i,j=1,\ldots,N} \left| d_{\square^m}(f(x_i), f(x_j)) - d_X(x_i, x_j) \right| \tag{22}$$

In MDS literature, the function σ which measures the distortion of distances is called *stress*. Historically, σ_2 has been used as the distortion criterion. Let us assume that $Z_i = f(x_i)$ is a matrix of canonical form coordinates and $d_{ij}(Z) = d_{\square m}(z_i, z_j)$, then:

$$\sigma_2(Z; D_X) = \sum_{i>j} \left| d_{ij}(Z) - d_X(x_i, x_j) \right|^2 \tag{23}$$

Here D_X is a matrix of geodesic distances and $d_{ij}(Z)$ is the Euclidean distance between the points on the canonical form. The minimization algorithms which minimize the stress function known as *Multidimensional scaling* (MDS). Historically, MDS has been classified as a dimensionality reduction method. SMACOF (scaling by majorizing a complicated function) is one of the well-known MDS algorithms for minimizing the stress function $\sigma_2(Z; D_X)$ with respect to Z. This algorithm was proposed by De Leeuw (De Leeuw 2005) is the core of our study in (Radvar-Esfahlan and Tahan 2011). We refer the reader to (Borg and Groenen 2005) for a detailed discussion on SMACOF algorithm. Despite its simplicity, the SMACOF guarantees a monotonically decreasing sequence of stress values. Fig. 2.4 illustrates the convergence of the SMACOF algorithm applied to the problem of embedding surface X (Fig. 2.3) sampled with N = 1511 points.

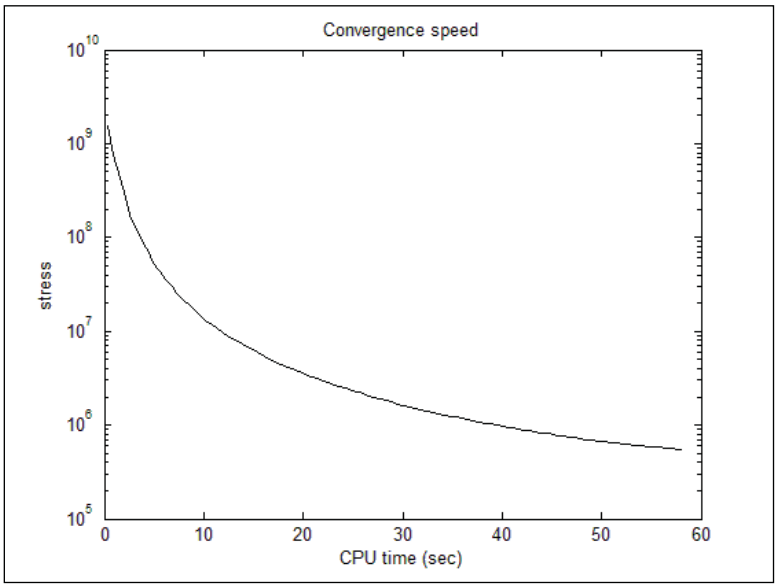

Figure 2.4 Convergence plot of SMACOF algorithm applied to shape X (Fig. 2.3) with N=1511 nodes

As discussed in (Radvar-Esfahlan and Tahan 2011) Euclidean embedding is rarely without distortion, especially if embedding is attempted for a surface that looks more like a sphere than like a plane into a Euclidean space. One way of overcoming this drawback is by choosing one of the surfaces, say *Y*, as the embedding space (Fig. 2.5). In other words, we would like to embed *X* into *Y* by solving the following problem:

$$\min_{y'_1,\ldots,y'_N \in Y} \sum \left| d_X(x_i, x_j) - d_Y(y'_i, y'_j) \right|^2 \tag{24}$$

where y'_i is the image of x_i in *Y*. Mathematical solution to this minimization problem on triangulated surfaces is known as *Generalized multidimensional scaling* (GMDS). We refer the reader to (Bronstein, Bronstein et al. 2006, Bronstein, Bronstein et al. 2007, Radvar-Esfahlan and Tahan 2011) for further accounts.

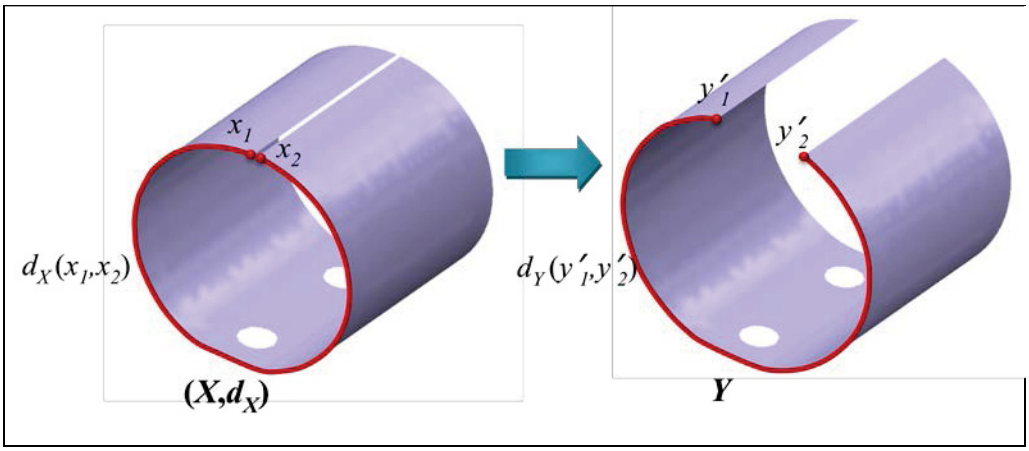

Figure 2.5 Generalized MDS

2.4.3 Incoherent geodesic distances

In this section, we discuss what we call *incoherent geodesics* and the origin of incoherency. Figs. 2.6a and 2.6b depict *X* and *Y* as two metric spaces corresponding to CAD model and range data. In Fig. 2.6a and in the middle of the part (white), consider an area with missing data. This is normally a common problem during the data acquisition process. Missing data can be caused by the operator's error or scanner precision. Data sampling and meshing can

also cause such a missing data region. While the actual geodesic between x_i and x_j in the CAD model is calculated by a straight (black) line, the geodesic in the range data (red dashed line) significantly varies from the nominal one (Fig. 2.6a). Fig. 2.6b depicts a case in which the operator decides to perform a partial inspection. In this case as well, the actual geodesic (red line) on the boundary of range data may vary from the nominal one (black line in the CAD model).

It should also be noted that in (Radvar-Esfahlan and Tahan 2011) we dealt with a very general case of inspecting a flexible part. We compared it with CAD-model. However in industry according to ASME Y14.5 and ISO 10579 normally use state (constraint state when joined with other parts) should be simulated. This kind of use state simulation can be considered as a special case of GNIF where some boundry conditions are known. In this study, we also use the boundary of the parts to perform the finite element non-rigid registration (section 3.4). However in most cases, the boundary of the parts is the most contaminated area with noise and geometric deviation. Thus, it may be another source of incoherency. So far, we know of two such geodesics: 1) those that have contact with the missing data region, and 2) others that have contact with the boundary of the scanned part. We will filter all these geodesics which we call *incoherent geodesics* out of the MDS procedure. In the next section the new method for contour detection will be presented.

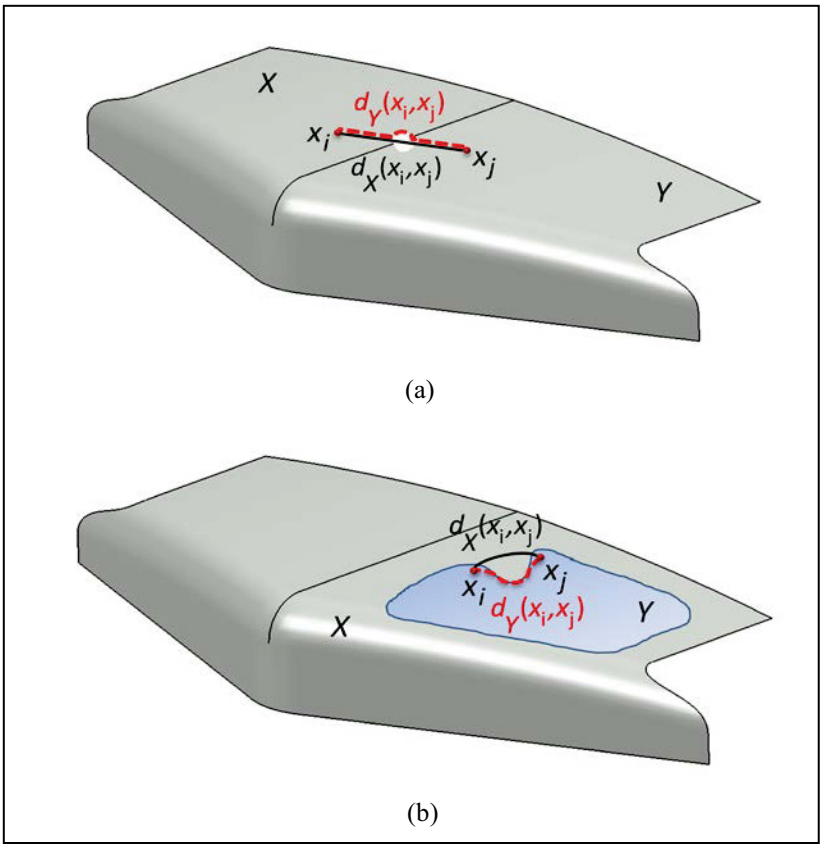

Figure 2.6 Incoherency caused by (a) missing data and (b) partial matching

2.4.3.1 Boundary detection

Geodesic distances are vital and critical as the inputs for the MDS algorithm. As discussed in previous section any incoherency can cause an inaccurate correspondence between CAD model and range data. To prevent such situations, we find all geodesics in contact with the mentioned regions and filter points causing such an incoherent geodesic distance. To this end, we propose a simple method for calculating the boundaries. Of course, as discussed in Section 2.2 there are many algorithms for edge and boundary detection in range data. Our method's simplicity comes from the ability of transforming the higher dimensional data into lower dimensional space.

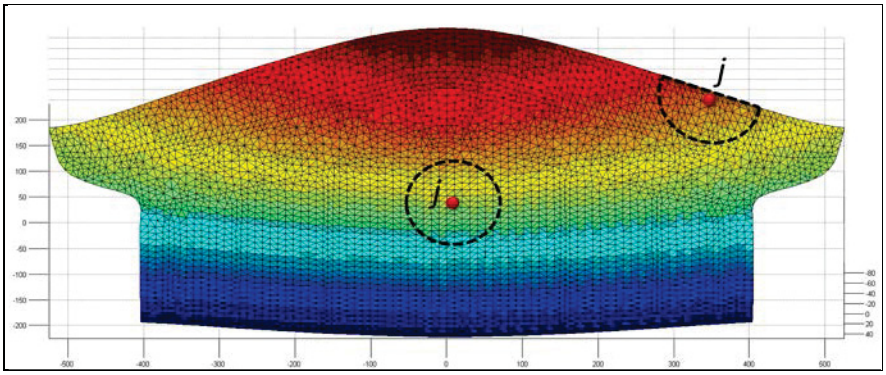

Figure 2.7 Boundary detection for the part in Fig. 2.6
(embedding using SMACOF)

In Fig. 2.7 any point j is a boundary point if all its neighbours are on one side of it. This simple idea leads us to following boundary detection algorithm:

Algorithm 2 Boundary detection algorithm

input: points cloud
output: boundary points (inner and outer)
1 **repeat** $\forall j \in \{1,...,N\}$
2 calculate the K nearest neighbours of the j
3 apply SMACOF algorithm to $K \times K$ matrix of nearest neighbours
4 calculate the center of gravity for K nearest neighbours
5 compute the *distance* between j and the center of gravity
6 **if** this *distance* is larger than some threshold **then** label it as boundary point

2.4.4 Finite element non-rigid registration

Our methodology is inspired by real industrial inspection processes. When the flexible part is placed on the inspection fixture, the prevailing idea is that we are going to simulate the *use state*; more specifically however, we can say that we are looking for some *correspondence* between the distorted part and the inspection fixture, which represents our CAD model. In (Radvar-Esfahlan and Tahan 2011) we presented a methodology based on the fact that the shortest inter-point path (geodesic distance) between any two points on a shape remains

unchanged during an isometric deformation. We called this property the *distance preserving property of non-rigid parts*. In Fig. 2.8, CAD model and range data are represented as a cantilever beam. For simplicity and without loss of generality, let us assume that some prior information about boundary conditions (e.g., support point) is already known. Rigid registration (e.g., ICP-based algorithm) can be done using this prior information. In the absence of plastic deformations, displacing x_1 to y_1 will deform the beam, and so there will be a bijective (one-to-one correspondence) distance-preserving map between these two shapes (by bijective we do not mean the exact nodal correspondence). Also, we assume that all pair-wise geodesic distances between the points on X (CAD model) and Y (scanned data) are available (e.g., using fast marching method). If we can introduce a similarity measure in order to find a correspondence between these two metric spaces, the step we call the *finite element non-rigid registration* (FENR) can be performed: (a) Find the correspondence (e.g., y_1 is the image of x_1); (b) Knowing some boundary conditions as prior information and finding the correspondence then displace x_1 towards y_1; (c) Calculate the geometric deviation between deformed CAD model and measure range data.

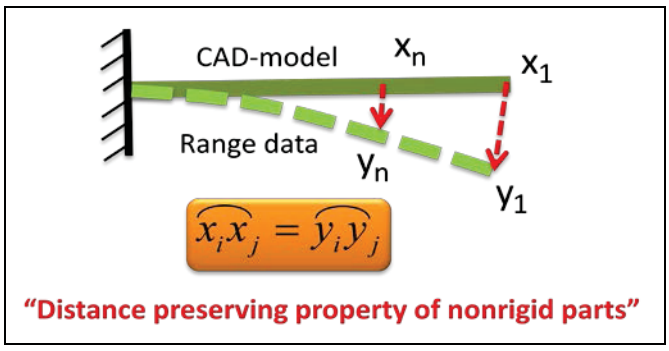

Figure 2.8 Finite element non-rigid registration

Notice that mapping the CAD model into range data has some advantages. Transforming the range data into a computer-aided analyzable model, especially for complicated surfaces, is a very-time consuming process. For such surfaces, more human intervention is needed. Furthermore, parts with hidden stiffening structures or other details on the back side of scanned surface, are very difficult to model as FEM-analyzable models. The main advantage

of the proposed method is that only one FEM-analyzable model should be created. This really decreases the inspection time, especially for mass production inspection.

2.5 Geometric inspection process

Detailed flowchart of our presented methodology is depicted in Fig. 2.9. Compared to GNIF (Radvar-Esfahlan and Tahan 2011), the main difference is to detect the incoherent geodesics in range data. Two kinds of incoherent geodesics have to be detected: those that have contact with the missing data region, and those that have contact with the boundary of the scanned part. Performing what introduced in Section 3.3.1 incoherent geodesics then have to be filtered out of GMDS algorithm. Then FENR step is applied to quantify the profile defect.

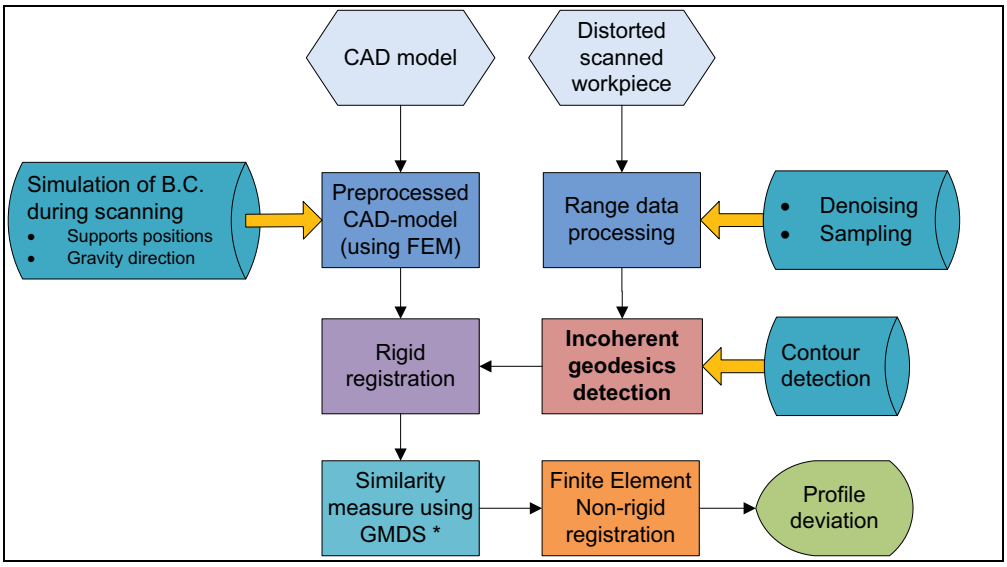

Figure 2.9 Inspection process flowchart using *RNIF*[5]

*Similarity measure can also be performed before rigid registration.

As GNIF, it should be noted that FENR was performed to quantify the amount of defect. Defect detection (visualisation) is completely possible without passing to this very time consuming stage. In fact in most cases of mass production it is desirable to find out where

[5] We refer the reader to Annex I for more details.

and when surface defects occur. Comparing two matrix of pairwise geodesic distances between CAD model and range data even visually can depict where the defect occurs.

Before going on to the next section it has to be noted that in this paper we assume the following:

1. The surface that is sampled is a valid surface.
2. There is a finite set of points that sample the surface.
3. There is no duplication of sampled points.
4. Any small perturbation of point locations does not change the connectivity in the reconstructed surface (Radvar-Esfahlan and Tahan 2011).
5. The different methods for meshing will not be discussed, and we assume that such (triangular) meshing exists for range data and the CAD surface.
6. The effect of the diverse smoothing methods in reducing the topological noise effect will not be discussed.
7. There is a bijective mapping between range data and the CAD model.

2.6 Results and discussion

We tested the presented methodology with four typical mechanical parts. Table 1 presents the overall size and engineering data. These case studies contain free forms, sharp edges, discontinuities (holes), and different sizes that evaluate the metrological (accuracy) performance of the method developed in the previous section. To this end, the free-form model was simulated by CATIA®, and a finite element analysis of the model was performed, simulating the free-state range data. At this step, a displacement and/or a force was applied to the model to simulate unknown deformation. Fig. 2.10 represents such a free-state simulation for the first case study. A predefined profile defect was also added to all case studies. For instance, Fig. 2.11 illustrates such a profile defect (8 mm maximum amplitude over a Ø200 mm area) for only one propeller blade.

Because we used predefined deformation in the range data generation steps (*deformation* and *profile defect*), qualitative performance evaluation is effectively traceable. Free-form and free-state point clouds were simulated with a different number of vertices to evaluate the

geodesic distance interpolation. We used a *Voronoi tessellation* to represent the sampled discrete nodes of the (metric) surface, after which incoherent geodesic detection was performed. To this end, we filtered out all the geodesics containing the inner and outer boundary points. In each part, we also added the regions with some missing data. After ICP-based rigid registration, similarity detection was performed using GMDS. The CAD model was then mapped to range data using detected points. Finally, the finite element non-rigid registration was performed. Here, only the maximum geometric deviation is presented (Table 2). For better visualization, a sampled tessellated section of the first case study with 50 sampled points is illustrated in Fig. 2.12. Geodesic distance interpolation enables us to accurately measure the similarity between the CAD and the scanned data, and there is still no exact nodal correspondence. In the rigid registration process, some prior defined points, or in the areas with the least defect probability, may be used to increase the procedure speed. As shown in Table 2, the primary GNIF results were significantly improved by the presented methodology (RNIF). This improvement is due to the capabilities presented by the filtering method. In fact, filtering the incoherent geodesic distances out of the multidimensional scaling process results in more accurate similarity measure detection.

Table 2.3 Case study size and engineering data

Case study 1 (wind turbine blade)	**Case study 2** (propeller)
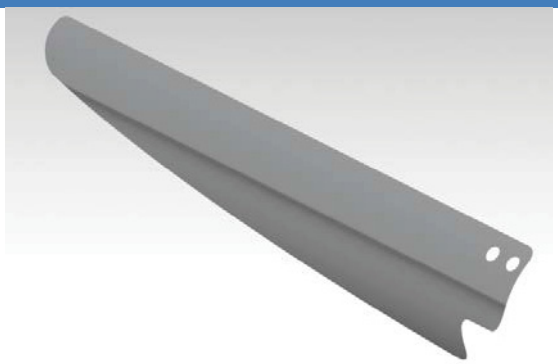	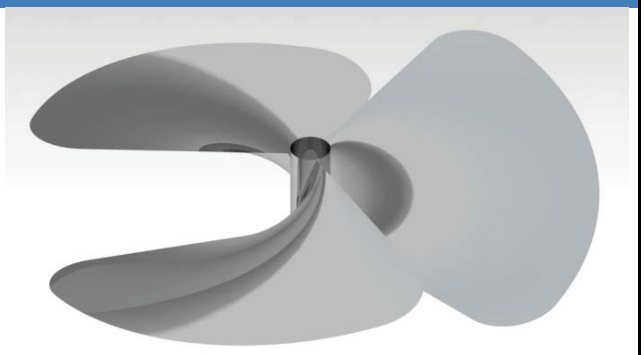
l =1200, r =150 (blade profile radius) Thickness =0.5 Aluminum	Φ860, Height =150 Thickness =0.5 Aluminum
Case study 3 (hood)	**Case study 4** (cover)
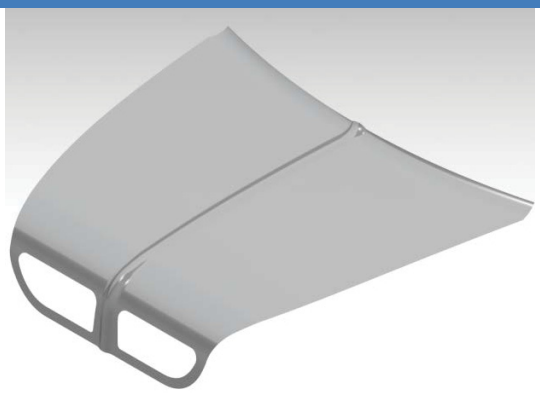	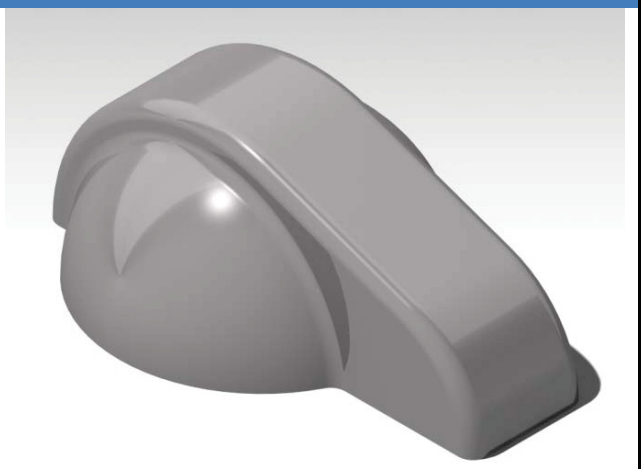
1900x1600x400 Thickness =0.5 Aluminum	600x400x225 Thickness =0.5 Aluminum

Note: Dimensions are in *mm*.

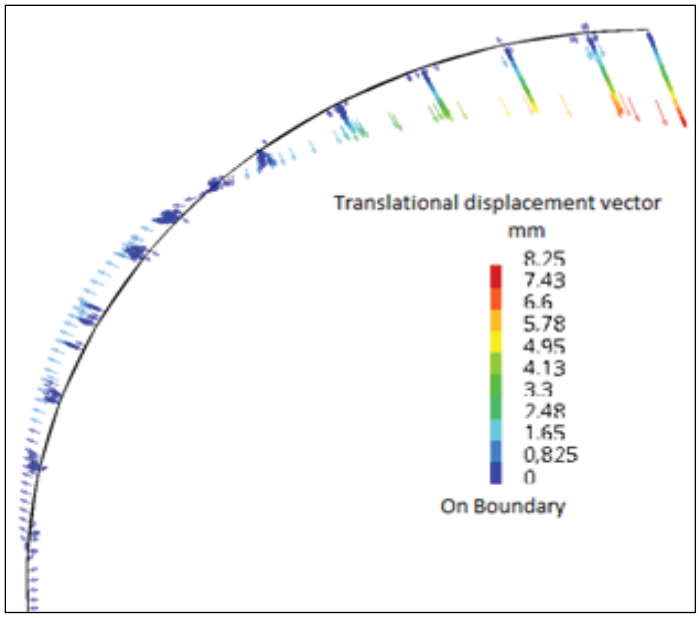

Figure 2.10 Predefined deformation for wind turbine blade (to simulate free-state) – Blade side view

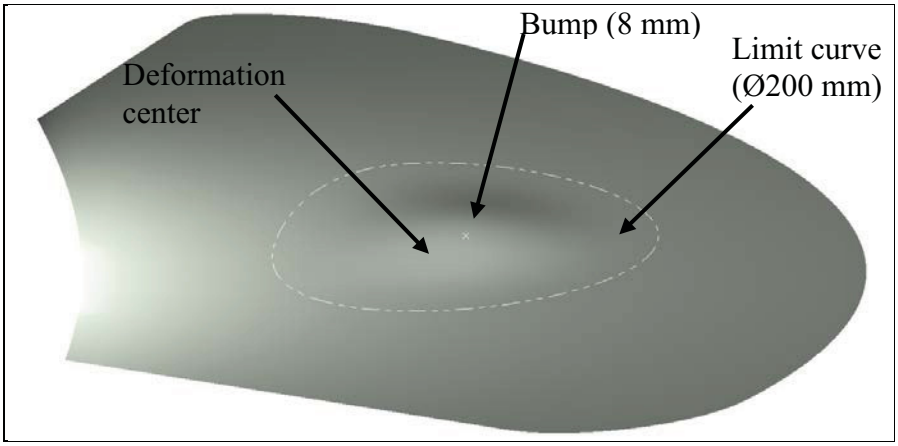

Figure 2.11 Sample predefined profile defect for Case study 2

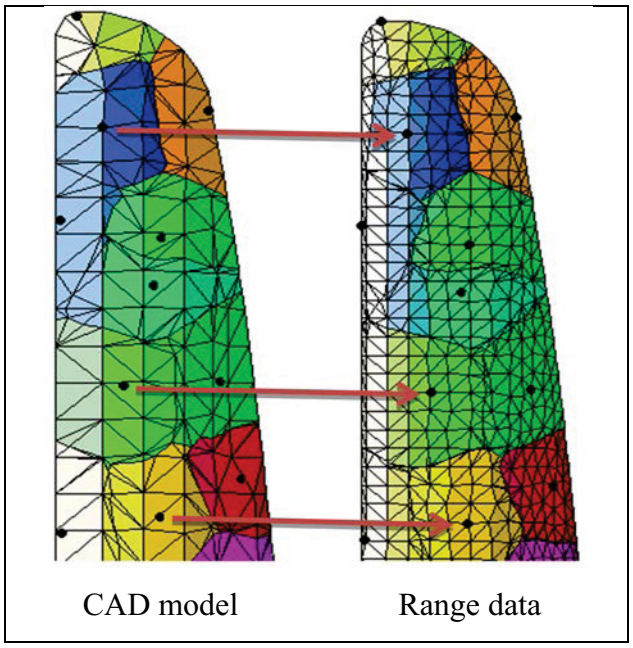

Figure 2.12 Similarity measure between CAD model and range data (with 1833 and 7140 nodes, respectively), End of turbine blade (Case study 1)

Table 2.4 Verification of RNIF

	Case study 1		**Case study 2**		**Case study 3**		**Case study 4**	
	GNIF	*RNIF*	*GNIF*	*RNIF*	*GNIF*	*RNIF*	*GNIF*	*RNIF*
Values identified by GNIF / RNIF	2.67[a] (50)[b] 2.85 (500) 4.57 (1500)	2.93 (50) 3.20 (500) 4.71 (1500)	5.07 (100) 7.67 (250) 7.90 (500)	5.98 (100) 7.73 (250) 7.95 (500)	3.00 (50) 5.02 (100) 6.47 (500)	3.73 (50) 6.11 (100) 6.91 (500)	2.09 (100) 6.95 (500) 9.19 (1000)	2.16 (100) 7.09 (500) 9.38 (1000)
Predefined profile deviation	5.00		8.00		7.00		10.00	

[a] All dimensions are in mm.
[b] The values between parentheses represent sampled points.

All case studies were performed on an AMD Phenom(tm) II X4 B95 Processor 3.00 GHz PC using a 64-bit operating system. For instance, the similarity measure in the first case study and for 50, 500 and 1500 sampled points took 1.2min, 9.9min and 117.8min, respectively. A correspondence search and the combination of the results with a non-rigid registration algorithm were the main computational demanding steps. As expected, increasing the density of sampled points led to more accurate results (see case studies by column in Table 2). On the one hand, to better represent the underlying surface deviation, we preferred to have the point sampling to be as dense as possible. On the other hand, we had to bear in mind that the discrete representation is used by computer algorithms, and every additional point increases storage and computational complexity costs.

2.7 Conclusion

Given the lack of theoretical knowledge and inspection methodology for non-rigid part inspection, the only method used to handle this problem today in industry involves using high cost inspection fixtures. In this study, we propose a robust foundation for a fixtureless non-rigid inspection. This research pioneers the inclusion of *part compliance* with *intrinsic geometry of surface* in the metrology of free-form surfaces. We introduced a new methodology based on the fact that the shortest path (geodesic distance) between any two points on a shape remains strictly unchanged during an isometric deformation. We called this property the *distance preserving property of non-rigid parts*. We merged the technologies in metric and computational geometry with nonlinear dimensionality reduction methods and finite element analysis to develop a general and robust approach to the geometrical inspection of non-rigid parts. Preliminary results proved that the proposed method, based on distance-preserving nonlinear dimensionality reduction methods (NLDR), was quite efficient. In the next study, we will develop and verify the proposed methodology with real-world tests in cooperation with our industrial partner. Also, in this study we did not deal with how the various smoothing methods reduce the topological noise effect. The uncertainty associated with the material properties was not examined. These methods, as well as the effect of material uncertainty, should also be studied in depth.

Another application of proposed methodology is to confirm the datums. According to ASME Y14.5-2009 a datum is a theoretically exact point, axis, line, plane, or combination thereof derived from the theoretical datum feature simulator. In most free-form parts datums are established by datum targets. A datum target is a specified point, line, or area of contact between the part and the machine surface, inspection equipment or a CAD model. It ensures that the part will be located the same way during both assembly and inspection. In most free-form shapes a critical question is how to confirm the datums. In this case, as discussed before, GNIF/RNIF as a framework for isometry-invariant partial surface matching can be used to verify the correspondence between selected datum areas between CAD model and captured point clouds.

The proposed method is not a perfect and faultless substitution for inspection fixtures and CMM reports. However, in real-time applications, it can be used for variational control of production lines; thereby removing the more need to stop production to test a workpiece. Although there are few research projects involving the geometric inspection of non-rigid parts, no general-purpose, fully automated and real-world practical method which can be a substitute for CMM reports exists. Specific long-term goals must be set and systematically accomplished.

CHAPITRE 3

PERFORMANCE STUDY OF DIMENSIONALITY REDUCTION METHODS FOR METROLOGY OF NONRIGID MECHANICAL PARTS

Hassan RADVAR-ESFAHLAN; Souheil-Antoine TAHAN

Laboratoire d'ingénierie des produits, procédés et systèmes (LIPPS)

École de technologie supérieure

Montreal, Canada, H3C 1K3

Article accepted for publication in « *International Journal of Metrology and Quality Engineering* »,

(October 2013)

3.1 Abstract

The geometric measurement of parts using a coordinate measuring machine (CMM) has been generally adapted to the advanced automotive and aerospace industries. However, for the geometric inspection of deformable free-form parts, special inspection fixtures, in combination with CMM's and/or optical data acquisition devices (scanners), are used. As a result, the geometric inspection of flexible parts is a consuming process in terms of time and money. The general procedure to eliminate the use of inspection fixtures based on distance preserving nonlinear dimensionality reduction (NLDR) technique was developed in our previous works. We sought out geometric properties that are invariant to inelastic deformations. In this paper we will only present a systematic comparison of some well-known dimensionality reduction techniques in order to evaluate their accuracy and potential for non-rigid metrology. We will demonstrate that even though these techniques may provide acceptable results through artificial data on certain fields like pattern recognition and machine learning, this performance cannot be extended to all real engineering metrology problems where high accuracy is needed.

Keywords: Computer Aided Inspection, Geometric inspection, Flexible parts, imensionality reduction.

3.2 Introduction

Geometric inspection, geometric modeling, range data acquisition and analysis have developed as separate fields of engineering among the various engineering and scientific communities. However, all these fields share common scientific concepts, and there are many missed opportunities because of a lack of mutual connection and wasted synergy. Computer-Aided Inspection is one of these connection points, while nonrigid geometric inspection shares a profound degree of understanding of all the mentioned disciplines. Currently, a flexible workpiece must be constrained or clamped during the measurement process in order to simulate the *use state*. To that end, expensive and special inspection fixtures need to be designed and manufactured (Abenhaim, Desrochers et al. 2012). On the other hand, some inspection stages cannot be fully automated with this conventional approach. As a result, the geometric inspection of flexible parts remains a time and money consuming process. Typically some inspection *set-up processes* for nonrigid parts in aerospace industry request over 60 hours of operations. Despite the multitude of papers and research that have been produced in the CAD, CAM and CAI fields, the inspection of flexible parts continues to pose difficulties and significant costs to industries because they need special fixation devices. This is also evidence of the lack of knowledge and theoretical foundations surrounding this special field. Our approach (Radvar-Esfahlan and Tahan 2010, Radvar-Esfahlan and Tahan 2011, Radvar-Esfahlan and Tahan 2011) was an effort to eliminate the use of special inspection fixtures in the metrology of flexible parts. We tried to provide a better understanding of the developed algorithms by having the comparison between different existing methods. We also added some techniques to robustify our *Generalized Numerical Inspection Fixture* (GNIF) (Radvar-Esfahlan and Tahan 2011). Our philosophy was based on the fact that the interpoint shortest path (geodesic distance) between any two points on the parts remains unchanged during an isometric deformation. We called this property *distance preserving property of nonrigid parts*. In fact GNIF was inspired by a real industrial inspection process. When a flexible part is put on an inspection fixture, the prevailing idea is that we are going to simulate the state of use. But more specifically, one can say that we are looking for some *correspondence* between distorted parts and inspection

fixtures, which represents our CAD-model. In spite of the accuracy of the presented methodology, the similarity detection process was extremely slow even for simple parts with zero Gaussian curvature.

In Section (2) a brief introduction to six NLDR methods will be presented concisely with theirs mathematical fundaments. Then in Section (3), described methods will be evaluated using some typical world engineering data. The aim is to illustrate a systematic comparison and precision for each method.

3.3 Dimensionality Reduction

Most problems in pattern recognition, such as image processing and speech recognition, begin with the preprocessing of high-dimensional signals. The complexity of most learning algorithms depends on the number of input dimensions D. This is why we are interested in reducing the embedding dimensionality with minimizing the loss of information, of course. In the literature there are two techniques for dimensionality reduction: *feature selection* and *feature extraction*. In feature selection the aim is to find d of D dimensions (where $d < D$) which gives us the most information. In other words, we are interested in finding the best subset of the set of the features. In metrology, feature selection is not a good approach for dimensionality reduction because the individual vertices do not carry much information on their own. It is the combination of vertices that provides the most discriminative information. This is the idea behind the feature extraction techniques. We therefore consider the following problem. Given a high dimensional data $X = (x_1, \ldots, x_n)$ where $x_i \in \mathbb{R}^D$ the aim is to compute the output data $Z_i \in \mathbb{R}^d$ that is the low dimensional representation of X. For techniques used in this paper only general information, including the steps for each method, will be included without going into derivation. Our focus in this paper is to compare the dimensionality reduction methods on the geometric metrology view point. Consequently, the aim is not to provide the details of the algorithms. We invite the reader to refer to the original paper of each algorithm for further details. However, we will sketch a concise summary of each algorithm for comparison and reference purposes. Next section deals with methods that

reduce the dimensionality of data by using distance and topology preservation as the criterion.

3.3.1 Distance Preserving DR techniques

For linear dimensionality reduction, some simple criteria like maximizing the variance preservation leads to one of the robust dimensionality reduction methods like *Principal Component Analysis* (PCA) (Jolliffe 2005). However, in nonlinear cases the use of the same simple criteria requires more complex data models. On the other hand, every manifold can be described by its pairwise point distances whether by Euclidean, graph or geodesics metrics. Tons of research has been undertaken and motivated by a simple fact: if close points are kept close and far points kept far, then the high dimensional data set and its low dimensional embedding share the same shape (Lee and Verleysen 2007). This section attempts to review some of the best-known existing methods.

3.3.1.1 Multidimensional Scaling (MDS)

Given the pairwise distance d_{ij} between *n* points and assuming that we don't know the exact coordinates of the points and how the distance is calculated, MDS (also known as Principal Coordinates Analysis (Gower 1966)) tries to place these points in low dimensional space in such a way that the Euclidean distance between them is as close as possible to d_{ij}. Historically, the most significant achievement on MDS begins with Torgerson's work in 1952 (Torgerson 1952). Before then, Young and Householder (Young and Householder 1938) used the Euclidean distance as a metric of similarity measure. Let X and Y be metric spaces and $f : X \to Y$ an arbitrary map. The *distortion* of f is defined by:

$$\text{dis } f = \sup_{a.b \in X} \left| d_Y(f(a), f(b)) - d_X(a,b) \right| \tag{25}$$

The distance $d_X(a,b)$ between a pair of points in X is mapped to the distance $d_Y(f(a), f(b))$ between the images of a and b under f (Burago, Burago et al. 2001). In our point cloud

setting, where the shape X is sampled at N points $X=\{x_1,\ldots,x_N\}$, the *distortion* criteria will be:

$$\sigma=\max_{i,j=1,\ldots,N}\left|d_{\square^m}(f(x_i),f(x_j))-d_X(x_i,x_j)\right| \tag{26}$$

In MDS literature, the function σ which measures the distortion of distances is called *stress.* Historically σ_2 is used as the distortion criterion. Assume that $Z_i=f\left(x_i\right)$ is a matrix of canonical form coordinates and $d_{ij}(Z)=d_{\square^m}(z_i,z_j)$, then:

$$\sigma_2(Z;D_X)=\sum_{i>j}\left|d_{ij}(Z)-d_X(x_i,x_j)\right|^2 \tag{27}$$

Here D_X is a matrix of geodesic distances and $d_{ij}(Z)$ is the Euclidean distance between the points on the canonical form. The minimization algorithms which minimize the stress function known as *Multidimensional scaling.* Historically MDS is classfied as a dimensionality reduction method. Scaling by Majorizing a COmplicated Function (SMACOF) is one of the well-known MDS algorithms for minimizing the stress function $\sigma_2(Z;D_X)$ with respect to *Z*. This algorithm was proposed by De Leeuw (De Leeuw 2005). This algorithm is the core of our study in (Radvar-Esfahlan and Tahan 2011). Here we present a brief introduction on SMACOF. We refer the reader to (Borg and Groenen 2005) for an account. Before summarizing the SMACOF algorithm, we describe some relations and notations. Equation (27) can be written in matrix form:

$$\sigma_2(Z;D_X)=tr(Z^TVZ)-2tr(Z^TB(Z;D_X)Z)+\sum_{i>j}d_X^2(x_i,x_j) \tag{28}$$

Here *V* is a constant $N\times N$ matrix with elements:

$$v_{ij}=\begin{cases}-1 & i\neq j\\ N-1 & i=j\end{cases} \tag{29}$$

and $B(Z;D_X)$ is an $N\times N$ matrix with elements:

$$b_{ij}(Z;D_X)=\begin{cases}-d_X(x_i,x_j)d_{ij}^{-1}(Z) & i\neq j \quad and \quad d_{ij}(Z)\neq 0\\ 0 & i\neq j \quad and \quad d_{ij}(Z)=0\\ -\sum_{i\neq k}b_{ik} & i=j\end{cases} \tag{30}$$

Thus, the SMACOF algorithm can be summarized as:

Algorithm 1 SMACOF algorithm

input: matrix of geodesic distances $[D_X]_{N\times N}$
output: canonical form Z*

1 set some initial $Z^{(0)}$ and $k = 0$
2 compute the raw stress $\sigma_2(Z^{(0)}; D_X)$
3 **repeat**
4 compute $Z^{(k+1)} = N^{-1}B(Z^{(k)}; D_X)Z^{(k)}$ (Guttman transform)
5 compute the stress for this iteration , $\sigma_2(Z^{(k+1)}; D_X)$
6 compute the difference
7 $k = k + 1$
8 **until** *convergence*
9 set $Z^* = Z^{(k)}$

Step 6 of SMACOF algorithm contains findings for the difference in the stress values between the two previous iterations. If it is less than some predefined tolerance, or if the maximum number of iterations has been reached, then the algorithm stops.

3.3.1.2 ISOmetric feature MAPping (ISOMAP)

This technique described by Tenenbaum *et al.*(Tenenbaum, De Silva et al. 2000) is the variant of MDS which uses graph distance (obtained by Dijkstra algorithm (Dijkstra 1959)) as an estimation of geodesic distance, and applies MDS to lower the dimension of input data. The ISOMAP technique can be summerized as:

Algorithm 2 ISOMAP algorithm

1 construct the graph of input data
2 calculate the shortest pairwise distance between all points
3 apply the MDS to the shortest path found in step 2

3.3.1.3 Maximum Variance Unfolding (MVU)

Weinberger *et al*. (Weinberger and Saul 2004) developed MVU algorithm (also known as Semidefinite Embedding) based on mapping the high dimensional data set into a low dimensional space that preserves the distance and angle between nearby input patterns. In MDS, the pairwise Euclidean distance of input date sets was used as they were. In ISOMAP, Euclidean distance was replaced by geodesic distance. In MVU, the transformation of distance is somehow more complicated than in MDS and ISOMAP. Distances are assumed to be preserved locally, while nonlocal distances are optimized in such a way that suitable embedding can be found. For instance, in 3D data sets the pairwise Euclidean distance is shorter than 2-dimensional embedding. Therefore MVU is considered to maximize the long distances while maintaining the shortest ones.

To this end, the aim of the MVU is to unfold data by maximizing pairwise distances, i.e.:

$$Max \sum_{ij} \left\| \vec{z}_i - \vec{z}_j \right\|^2 \tag{31}$$

subject to

$$\forall (i, j) \in edges; \quad \left\| \vec{x}_i - \vec{x}_j \right\|^2 = \left\| \vec{z}_i - \vec{z}_j \right\|^2 \tag{32}$$

and

$$\sum_i \vec{z}_i = \vec{0} \tag{33}$$

The latter constraint was put in place to eliminate translational degrees of freedom in the lower space by centering the output on the origin. The aforementioned optimization objective is a non-convex problem (multiple local minima) because it means maximizing a quadratic form subject to quadratic equality constraints. In (Weinberger and Saul 2004) the authors propose a *Semidefinite Programming* (Vandenberghe and Boyd 1996) technique by using dot products instead of squared distances. If D denotes the square matrix of squared Euclidean distances, and K the *Gram matrices* of X; i.e. $K_{ij} = x_i.x_j$, without going into detail, the MVU algorithm can be summarized as follows:

Algorithm 3 MVU algorithm

1 Compute all squared pairwise distances in matrix D
2 determine the k-nearest neighbours G, of each data point
3 find *Max trace*(K) subject to:

$$k_{ii} + k_{jj} - 2k_{ij} = \left\| x_i - x_j \right\|^2 \quad for \quad \forall (i,j) \in G$$

$$\sum_{ij} k_{ij} = 0$$

$$K \geq 0$$

4 perform classical metric MDS on matrix K

3.3.1.4 Sammon's Mapping

The main weakness of MDS is that it tries to maintain large pairwise distances and does not retain the small ones (Van der Maaten, Postma et al. 2009). *Sammon' Mapping* (SM) (Sammon Jr 1969) tries to overcome MDS' weakness by weighting the contribution of each pair. To this end, SM minimizes the following stress function:

$$E_{SM} = \frac{1}{\sum_{ij} d_X(i,j)} \sum_{\substack{i=1 \\ i<j}} \frac{(d_X(i,j) - d_Z(i,j))^2}{d_X(i,j)} \tag{34}$$

where d is measured by Euclidean metrics. The minimization of Sammons's stress function can be performed using a pseudo-Newton optimization method.

3.3.1.5 Curvilinear Component Analysis (CCA)

Originally developed by Demartines and Herault (Demartines and Hérault 1997), *Curvilinear Component Analysis* (CCA) is an improvement of Sammon's mapping. This technique combines some of the attitudes of SM and MDS along with artificial neural network strategies in order to map the higher dimensional data to lower dimensional space. At first, CCA processes a vector quantization step (Gersho and Gray 1992) as a way to reduce the data set size. Then, like MDS, the authors defined a *stress* function in such a way as to preserve the interpoint distances during mapping. The CCA stress function closely resembles Sammon's stress function:

$$E_{CCA} = \frac{1}{2}\sum_{i=1}^{N}\sum_{j=1}^{N}\left\{d(x_i, x_j) - d(z_i, z_j))^2 F_\lambda(d(z_i, z_j)\right\} \quad (35)$$

While we would like to have $d(x_i, x_j) = d(z_i, z_j)$, this is not always possible without distortion, so they introduced a weighting function F_λ. The choice of F_λ is based on the fact that preserving the short distances is more significant than the longer ones, because the long distances on the manifold have to be stretched to unfold the manifold. Thus, F_λ was choosing as monotically decreasing function (Gersho and Gray 1992). In order to minimize cost function, Demartines and Herault (Demartines and Hérault 1997) developed a novel variant of gradient descent techniques. We refer the reader to their original work for an account. In our study we didn't sampled the range data. Therefore, the vector quantization is considered an optional processing. Curvilinear Distance Analysis (CDA) developed by Lee *et al.* (Lee, Lendasse et al. 2002) is considered a variant of CCA which uses graph distance instead of Euclidean distance.

3.3.2 Topology preserving techniques

As depicted in the previous section, dimensionality reduction can be reached by distance preservation. In this category numerous methods were discussed. While the comparative distances seem to give sufficient information on manifold, most distance functions make no distinction between manifold and its surrounding space. Topology preserving methods are another class of dimensionality reduction techniques that tend to preserve important structures of the data in the geometric structure of the mapping. One simple example of topology preserving maps is a Mercator projection of the earth into 2D space. While this kind of mapping gives invaluable visual information, distortion can't be prevented in some areas. In metrology, the topology gives the neighbourhood relationship between defect areas and the rest of the shape. The most problematic area in topology preserving techniques is how to represent a topology. All physical objects subjected to metrology are continuous. Unfortunately, continuous topology representation is not always possible. This is why discrete representation is used by a '*lattice*' (or *grid*). In this category we have selected the most well-known technique which we will summarize in the next section.

3.3.2.1 Locally Linear Embedding (LLE)

Locally linear embedding (Roweis and Saul 2000) is an eigenvector based technique (like PCA and MDS) where optimization doesn't involve local minima and iterative optimizations. It tries to preserve the local angles. LLE supposes that each point with its neighbors on the manifold lies on, or close to, a locally linear patch. Then it tries to characterize the local geometry of the patches by finding linear coefficients that reconstruct each point by using its *k*-nearest neighbors. Saul and Roweis (Roweis and Saul 2000) measured the reconstruction error by :

$$\varepsilon(w) = \sum_i \left| x_i - \sum_j w_{ij} x_j \right|^2 \tag{36}$$

where x_j is the *k*-nearest neighbors of x_i. w_{ij} summarizes the contribution of the *j*th data point to the *i*th reconstruction and are found by optimizing the equation (12) subject to $\sum_j w_{ij} = 1$. The authors found optimal weights by using a least squares method. The final step of the algorithm is to reconstruct a representation z_i of the x_i in a low dimensional space. This was performed by minimizing the embedding cost function:

$$\Phi(z) = \sum_i \left| z_i - \sum_j w_{ij} z_j \right|^2 \tag{37}$$

The authors also proposed a sparse eigenvector problem in order to minimize the aforementioned cost function. We refer the reader to LLE's original paper for more details on the minimization technique.

The comparison of DR methods on *Pattern classification* and *Data visualization* can be found in (Yin 2007, de Medeiros, Costa et al. 2011).

3.4 Experiment and results

In the previous section we summarized some well-known NLDR techniques. In this section, the systematic comparison of the methods, along with their accuracy (minimum correspondence error) and performance in typical mechanical parts, will be investigated. To

this end, we have categorized the very real engineering problems to four groups. Flexible parts with:

1) Zero Gaussian curvature with sharp edge (study case A);

2) More complex shape with mostly zero Gaussian curvature (study case B);

3) Free-form high curvature (study case C);

4) Combination of both (study case D).

The aim of this study is to investigate the performance of NLDR methods on nonrigid parts from the viewpoint of metrology. To this end, all case studies (CAD-model & range data) are considered to be intrinsically similar (Radvar-Esfahlan and Tahan 2010). This means that all case studies considered are geometrically defectless. Figure 3.1 illustrates four case studies investigated for this study. The models were created by CATIA® V5. Afterwards, a finite element analysis of the model was performed to simulate the free-state range data. At this point, a displacement and/or a force were applied to the model to simulate spring back deformations. Then arbitrary translational and rotational displacements were added to the range data. In this way, the CAD-model and range data were simulated in different coordinate systems. Table 3.1 represents the geometric and mechanical properties of the case studies.

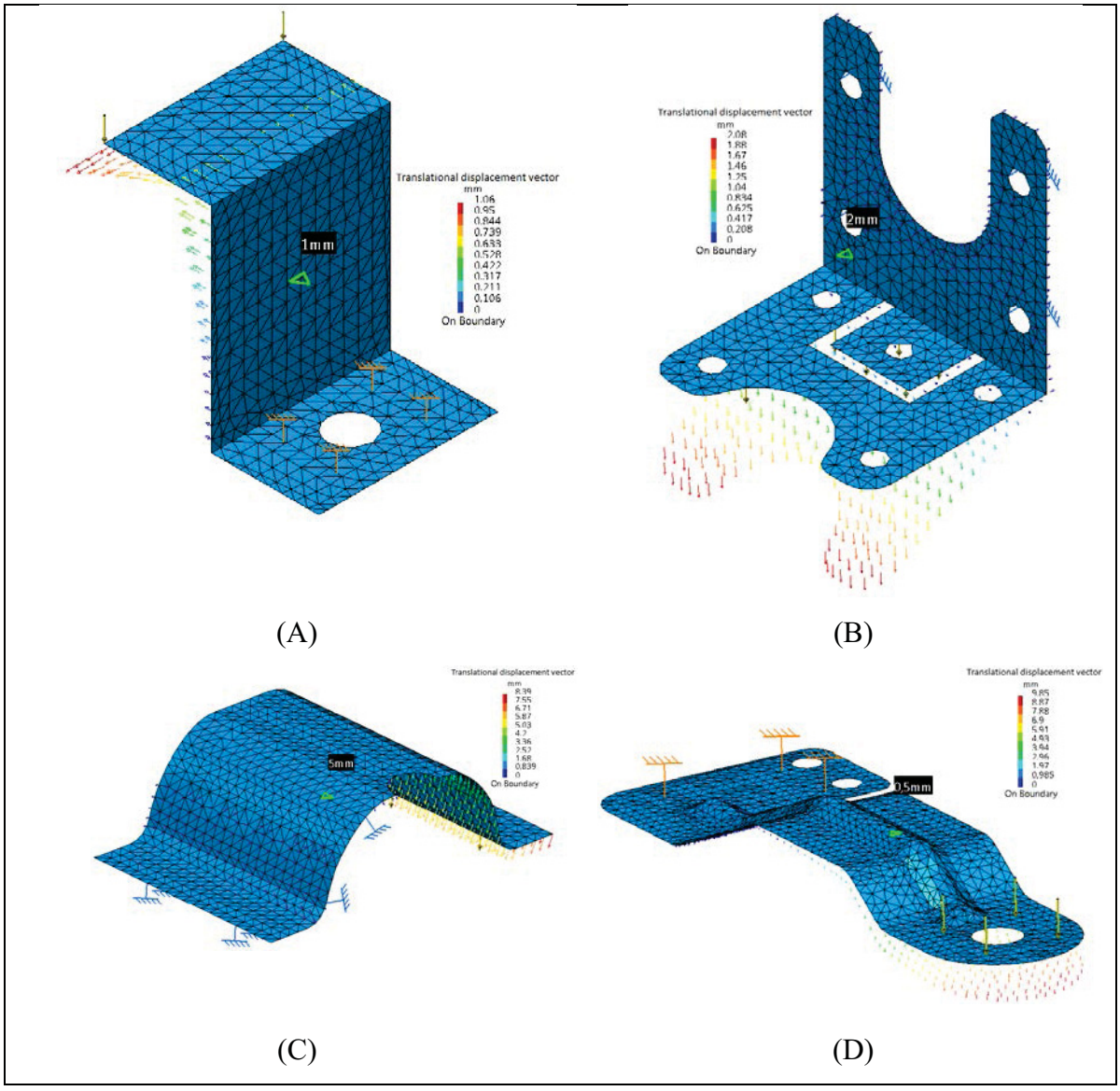

Figure 3.1 Study cases

Table 3-1 Geometric and mechanical properties of case studies

Case study	Material	Thickness [mm]	Dimension [mm]	# of nodes
A	Al-6061-T6	1.0	120x120x100	496
B	Al-6061-T6	2.0	100x100x80	701
C	Al-6061-T6	5.0	1600x1000x450	996
D	Al-6061-T6	0.5	340x130x50	1322

In order to compare similarities between the CAD-model and range data after reducing the dimensionality, a Procrustes analysis was performed. Then the Euclidean distances between all corresponding points have been calculated. As an instance the performance study on the case study D is presented in Figure 3.2. All case studies were performed on an AMD Phenom(tm) II X4 B95 Processor 3.00GHz PC using a 64-bit operating system. Table 3.2 demonstrates the computational time for each NLDR algorithm. The results of the analysis as *mean* (Accuracy) and *standard deviation* (Precision) for all study cases were illustrated in Table 3.3. The effect of registration error is considered to be equal for all case studies.

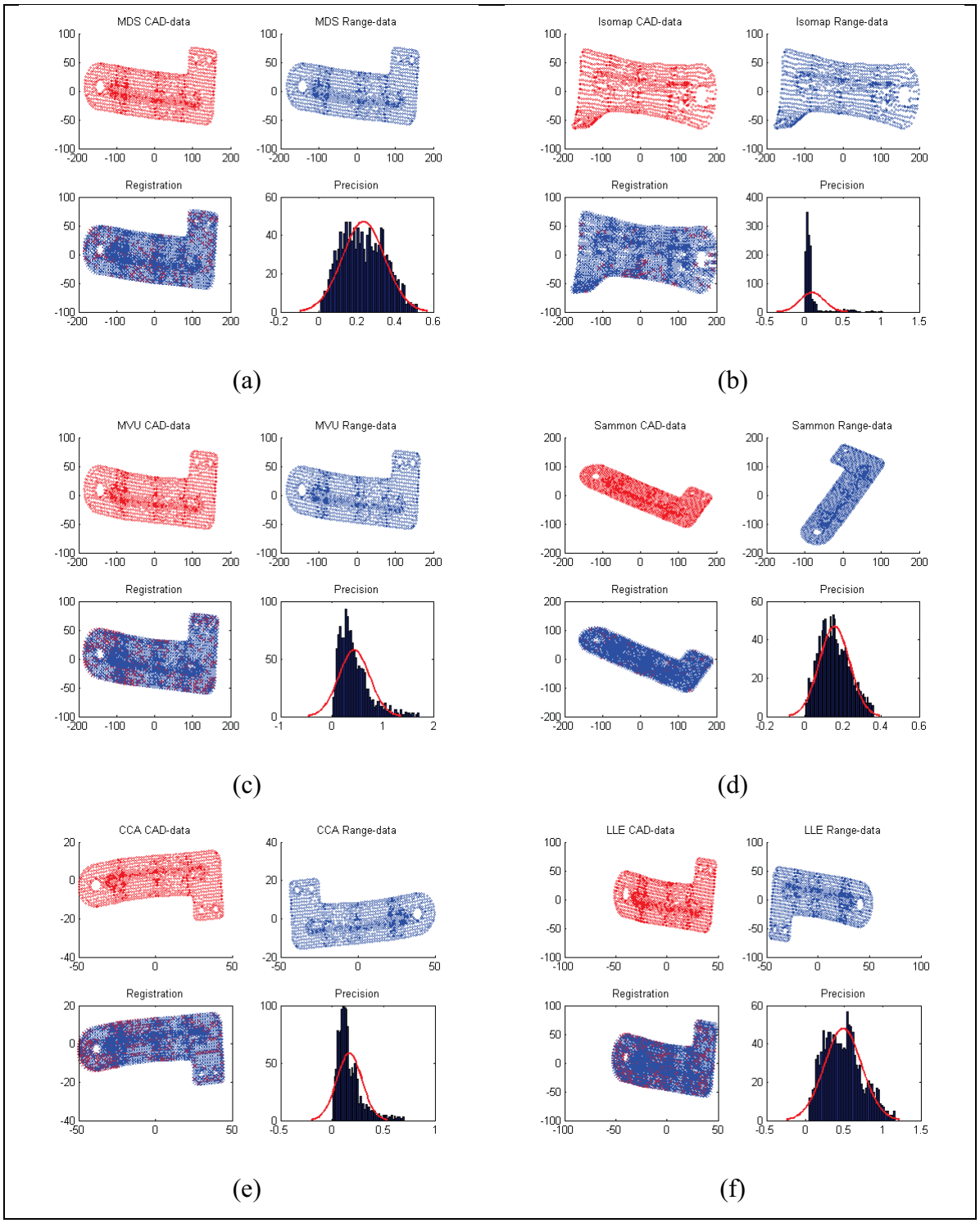

Figure 3.2 2D embedding of case study (D) using:
(a) MDS; (b) ISOMAP; (c) MVU; (d) SM; (e) CCA; (f) LLE.

Table 3-2 Computational time [sec]

Case study	MDS	ISOMAP	MVU	SM	CCA	LLE
(A)	0.371	15.596	0.930	16.493	1.050	0.789
(B)	0.782	33.202	3.073	40.840	2.236	1.097
(C)	1.096	72.249	4.086	106.172	3.788	2.346
(D)	1.912	140.833	6.004	297.410	5.345	4.525

Table 3-3 Mean and Standard deviation

Case study		MDS	ISOMAP	MVU	SM	CCA	LLE
(A)	**mean**	0.09	1.78	1.95	0.056	0.86	1.18
	std	0.06	1.42	0.99	0.03	0.44	0.78
(B)	**mean**	0.29	0.30	0.14	0.18	0.08	3.84
	std	0.16	0.17	0.10	0.07	0.06	2.38
(C)	**mean**	0.61	0.38	11.56	0.47	0.44	12.15
	std	0.26	0.23	10.24	0.19	0.64	8.52
(D)	**mean**	0.23	0.10	0.44	0.16	0.17	0.50
	std	0.11	0.16	0.30	0.08	0.12	0.24

Table 3-4 Overall performance of NLDR methods in metrology

	Study case A	Study case B	Study case C	Study case D
MDS	★★★★	★★	★★	★★
ISOMAP	★★	★	★★★★	★★★★
MVU	★	★★★	★	★★
SM	★★★★	★★★	★★★	★★★
CCA	★★★	★★★★	★★★	★★★
LLE	★★	★	★	★

3.5 Discusion

According to the results of means and standard deviations, Table 3.4 illustrates the overall performance of dimensionality reduction methods for each study case. For free form high curvature parts (Study case C), a graph distance based ISOMAP perform better than other methods. This is something we already expected. In (Radvar-Esfahlan and Tahan 2010,

Radvar-Esfahlan and Tahan 2011, Radvar-Esfahlan and Tahan 2011) the authors used geodesics instead of graph distance as a similarity measure. However experiments shows that ISOMAP stands behind Sammon's nonlinear mapping as one of the computationally high casting methods. Classical MDS can be effectively used in simple parts with zero Gaussian curvature. On the other hand, classical MDS stands to be the fastest among the others. The performance of ISOMAP is notably worse than classical MDS in cases where parts have zero Gaussian curvature with sharp corners. The reason behind this phenomenon is the error of the geodesic/graph distance computation where the sharp bends occur. However, where the complexity increases (in the absence of sharp bends), ISOMAP offers more chances to achieve good precision. Although MVU uses the graph distance, it doesn't perform in the same manner as ISOMAP. Classical scaling cost functions used by Isomap retain the large geodesic/graph distances, while MVU focuses on keeping the local/small structure data. MVU should be avoided in the case of free form highly curved parts with large deformations where the curvature changes instantly.

Unlike classical MDS and MVU, Sammon's mapping can effectively handle all kinds of linear and nonlinear manifolds. While its global convergence is not always guaranteed it is also the most time-consuming NLDR technique.

By comparison, CCA proves to be much more flexible and can handle most linear and nonlinear data sets mostly because it gives the user the possibility of choosing the weighting function F_λ. In spite of the fact that CCA's cost function is mostly like Sammon's mapping, its convergence is faster.

The results of our experiments show that in spite of LLE's simplicity (there are only two parameters to be set); this topology preserving technique doesn't outperform the distance preserving techniques. In fact, the performance of LLE is somehow disappointing for the majority of real-world parts. LLE suffers from a fundamental weakness in its cost function (Chen and Liu 2011).

3.6 Conclusion

With (Radvar-Esfahlan and Tahan 2010, Radvar-Esfahlan and Tahan 2011, Radvar-Esfahlan and Tahan 2011) the authors have pioneered the concept of dimensionality reduction methods in 3D geometric metrology. In this paper we presented a review and systematic comparison between NLDR methods in order to evaluate their performance for applications on the metrology of flexible parts. We showed that even though these techniques may give acceptable results by artificial data on some fields like pattern recognition and machine learning, their performance cannot be extended to real engineering problems such as geometric metrology where high accuracy is needed. In spite of their undeniable performance for the metrology of flexible parts, special attention should be paid to each case for selecting the particular nonlinear dimensionality reduction technique.

CONCLUSION

In-depth bibliographical research shows that for the geometric and dimensional inspection of nonrigid parts using range data, a general-purpose, fully automated and practical method doesn't yet exist. Even today, our industrial partner *Bombardier Aerospace* and *Creaform 3D* use special fixtures (jig) with CMM to inspect flexible parts. This inspection method typically requires 60 hours of operations. While 3D scanning devices allow for a quick and economic point cloud generation in high precision, registration and measuring processes using these kinds of scanners cause certain difficulties in industry in the case of nonrigid parts.

In this thesis we developed and proposed a theoretical foundation along with a novel concept for the fixtureless geometric inspection of nonrigid parts. Including part compliance with the intrinsic geometry of surface is an area of research pioneered with this thesis as a solution to the industry's increasing problems in the field of nonrigid metrology. We introduced a comprehensive methodology based on the fact that the shortest path (geodesic distance) between any two points on a shape remains unchanged during an isometric deformation. We call this property a *distance preserving property of nonrigid parts*. We merged the technologies in metric and computational geometry along with nonlinear dimensionality reduction methods and finite element analysis to develop a general approach to the geometrical inspection of flexible parts. The preliminary results proved that the proposed methods, based on distance preserving NLDR methods were quite efficient.

This thesis was advanced in three chapters. In Chapter 1, we sought out the intrinsic geometric properties which are invariant to isometric deformations. We used geodesics as a similarity measure. Then we used these similarities for nonrigid finite element registration between CAD-model and range data. We called this technique the GNIF (Radvar-Esfahlan and Tahan 2011). In fact GNIF was the numerical replacement of traditional inspection fixtures. Then in Chapter 2, we tried to robustify the GNIF by filtering some incoherent geodesics out of similarity detection algorithm. We did not even think that the mission was accomplished by robust GNIF. In Chapter 3, we presented a systematic comparison of some

well-known dimensionality reduction techniques in order to evaluate their accuracy and potential for non-rigid metrology. Special kinds of mechanical flexible parts, i.e., parts with zero Gaussian curvature were also discussed in Chapter 3.

Originality of the thesis

The significant contributions made by this thesis include the following:

1) A comprehensive system was developed for the geometric inspection of nonrigid parts. *Bibliographical research shows that we are the first to introduced concept of intrinsic surface geometry in order to simulate the inspection process of flexible (deformable) parts.*

2) Unlike the methods presented by other authors which were the subject of discussion in Chapter 1, *for the embedding process, to find the similarity between a CAD-model and range data (two different metric spaces), there is no need for primary surface registration*. This really speeds up the measuring process, especially when we have prior information about the assembly process.

3) More recently, Jaramillo *et al.* (2013) tried to handle the problem of nonrigid inspection using partial captures. *In fact one of the significant specifications of GNIF (Radvar-Esfahlan and Tahan 2011) was the capability for isometry-invariant partial surface matching*.

4) *Large deformations* are completely normal for more flexible parts. Where appropriate, large deformations were involved in the case studies. Then GNIF was implemented and tested. The results were encouraging.

5) During this research we were looking to quantify the amount of profile defects. Thus, it should be noted that FENR was performed to quantify the amount of defect. *Defect detection is completely possible without passing to this very time consuming stage*. In fact in most cases of mass production it is desirable to find out where and when

surface defects occur. Comparing two matrix of pairwise geodesic distances between CAD model and range data even visually can depict where the defect occurs.

6) So far all the parts we dealt with were sheet metal. *However it should be noted that GNIF/RNIF can be successfully applied to the parts with hidden stiffening structures (variable flexibility)*. In fact any FEM-analysable CAD model/material can be used for embedding the FENR process. The beauty of this presented methodology is that, this was a CAD model which was mapped into range data and not vice-versa.

7) It should also be noted that we dealt with a very general case flexible (deformable) part inspection. We compared it with a CAD-model. However in industry according to ASME Y14.5 and ISO 10579 normally a *use state* (constraint state when joined with other parts) should be simulated. This kind of use state simulation can be considered a special case of GNIF where some boundry conditions are known.

8) According to ASME Y14.5-2009 a *datum* is a theoretically exact point, axis, line, plane, or combination thereof derived from the theoretical datum feature simulator. In most free-form parts datums are established by datum targets. A *datum target* is a specified point, line, or area of contact between the part and the machine surface, inspection equipment or a CAD model. It ensures that the part will be located the same way during both assembly and inspection. In most free-form shapes a critical question is how to confirm the datums. In this case, as discussed before, GNIF as a framework for isometry-invariant partial surface matching can be used to verify the correspondence between selected datum areas between CAD model and captured point clouds.

RECOMMENDATIONS

Although we have tried to present convincing results, no method with such promise is likely to be widely accepted until more practical testing can be done. Several topics that should be investigated further arose during the course of this research.

1) The developement of more accurate geodesic distance calculation in triangulated surfaces should be absolutely considered for future research.

2) More in-depth research would involve the study of uncertainties and their propagation. Metrology variables can be divided into two categories: material variables (e.g. yield strength and ultimate strength) and geometry variables (e.g. pairwise geodesic distance and plate thickness). The accuracy of the GNIF is limited by measurement uncertainty. The measurement uncertainty is the sum of the uncertainty of the following items:

    - Uncertainty of data acquisition system (scanner).
    - Uncertainty of denoising filters.
    - Uncertainty in the simulation of the fixation system.
    - Uncertainty of pairwise geodesic distance calculation (FMM).
    - Uncertainty of GMDS and other NLDR methods.
    - Uncertainty of FENR.
    - Uncertainty of material variables (e.g., Young's modulus, yield strength)

3) In this thesis we developed the theoretical foundation for the metrology of flexible parts. However the research can be criticized due to a lack of practical experiments. Currently Mr. Vahid Sabri (Ph.D. candidate at École de technologie superieure) tries to fill this gap with practical tests. In (Sabri, Tahan et al. 2013) the authors successfully applied GNIF to a real case study involving our industrial partner (Bombardier Aerospace) (Fig. 0.2). The results were encouraging.

4) According to ASME Y14.5.1M-1994 a profile tolerance zone is an area (profile of line) or a volume (profile of surface) generated by offsetting each point on the nominal surface in a direction normal to the nominal surface at that point. Thus, a geometric deviation for a point can be defined as a deviation measured normal to the tolerance zone. While this definition was applied to all dimensioning and tolerancing applications during the last decades, we believe that this definition can be modified according to the technological advances in numerical data capturing systems using CMM/Scanners. This thesis demonstrated that point to point correspondence between a CAD model and scanned data are precisely accessible. Thus, a point's geometric deviation can be defined as spatial-point-to-point distance between a specific point on range data and its correspondence on the CAD model. We believe that for the case of very flexible parts the conventional deviation identification should be modified.

5) Although this research did not cover the GD&T discussions (tolerancing), the author was engaged to this interesting area as a hand-on-operation engineer during most his carrier. GD&T defines itself as a system for defining and common communication language on engineering specifications and tolerances. The core of this standard evolved around pass/fail inspection by Go/No Go gaging (Maximum and Least Material Conditions: MMC & LMC). Even in its latest edition (ASME Y14.5-2009) this standard stands far behind the technological evolution on modern statistical based practices such as probabilistic tolerance analysis methods and advances in range data capturing devices. However we find wide range of softwares claiming statistical analysis for deformable parts while there is no consensus as what the right approach is. We invite researchers for more focusing to this abandoned area.oned area.

ANNEX I

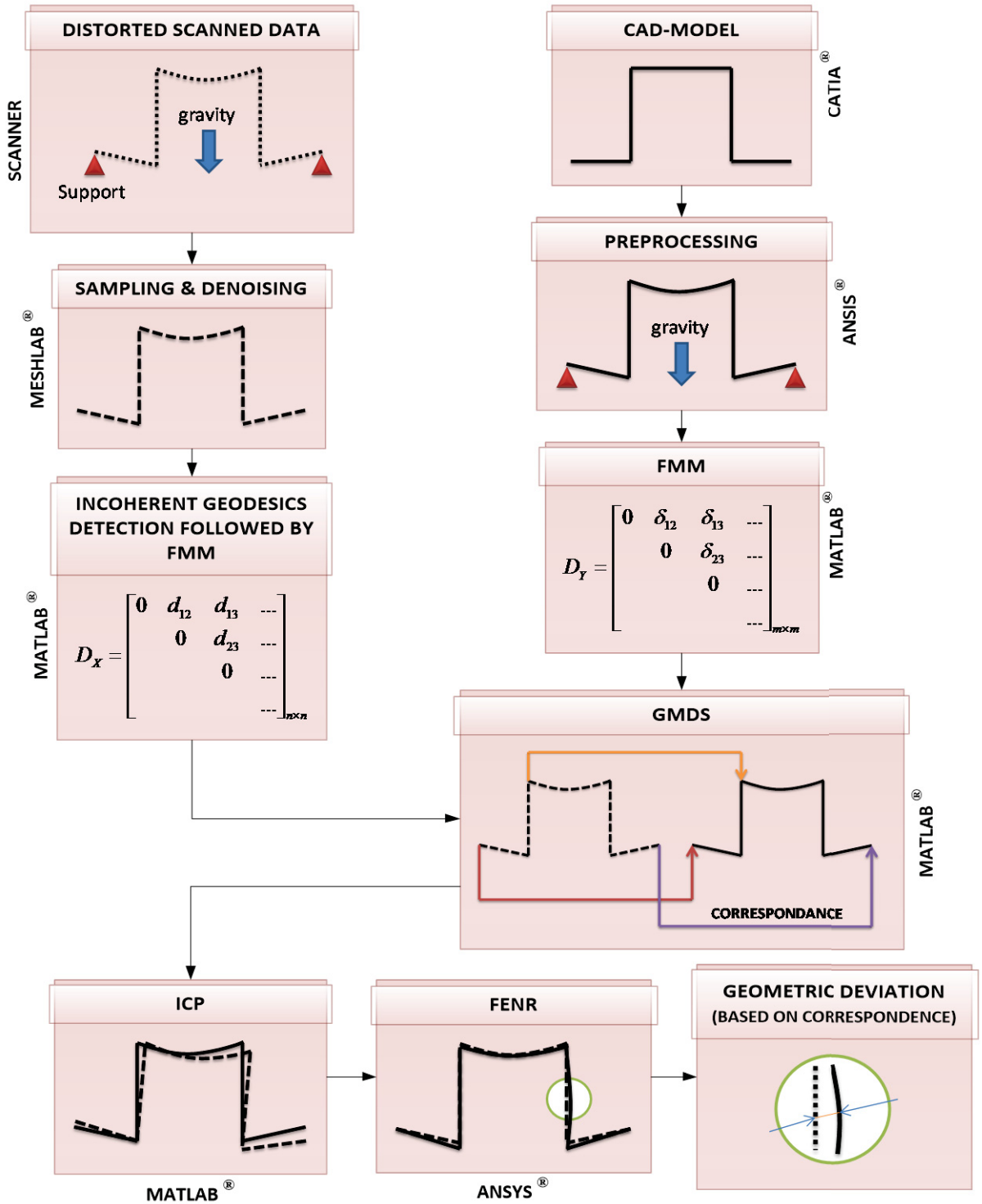
DISTORTED SCANNED DATA
SCANNER
gravity
Support
SAMPLING & DENOISING
MESHLAB®
INCOHERENT GEODESICS DETECTION FOLLOWED BY FMM
MATLAB®
$D_X = \begin{bmatrix} 0 & d_{12} & d_{13} & \cdots \\ & 0 & d_{23} & \cdots \\ & & 0 & \cdots \\ & & & \cdots \end{bmatrix}_{n\times n}$
CAD-MODEL
CATIA®
PREPROCESSING
gravity
ANSIS®
FMM
$D_Y = \begin{bmatrix} 0 & \delta_{12} & \delta_{13} & \cdots \\ & 0 & \delta_{23} & \cdots \\ & & 0 & \cdots \\ & & & \cdots \end{bmatrix}_{m\times m}$
MATLAB®
GMDS
CORRESPONDANCE
MATLAB®
ICP
MATLAB®
FENR
ANSYS®
GEOMETRIC DEVIATION
(BASED ON CORRESPONDENCE)

BIBLIOGRAPHY

Abenhaim, G., S. Tahan, A. Desrochers and R. Maranzana (2011). "A novel approach for the inspection of flexible parts without the use of special fixtures " ASME, Journal of manufacturing science and engineering.

Abenhaim, G. N., A. Desrochers and A. Tahan (2012). "Nonrigid parts' specification and inspection methods: notions, challenges, and recent advancements." The International Journal of Advanced Manufacturing Technology **63**(5-8): 741-752.

Alrashdan, A., S. Motavalli and B. Fallahi (2000). "Automatic segmentation of digitized data for reverse engineering applications." IIE transactions **32**(1): 59-69.

Amberg, B., S. Romdhani and T. Vetter (2007). Optimal step nonrigid ICP algorithms for surface registration, Citeseer.

Anguelov, D., B. Taskar, V. Chatalbashev, D. Koller, D. Gupta, G. Heitz and A. Ng (2005). "Discriminative learning of markov random fields for segmentation of 3d scan data."

Bentley, J. (1975). "Multidimensional binary search trees used for associative searching." Communications of the ACM **18**(9): 517.

Besl, P. and H. McKay (1992). "A method for registration of 3-D shapes." IEEE Transactions on pattern analysis and machine intelligence **14**(2): 239-256.

Borg, I. and P. J. F. Groenen (2005). Modern multidimensional scaling: Theory and applications, Springer Verlag.

Bourdet, P. and A. Clément (1976). "Controlling a complex surface with a 3 axis measuring machine." Annals of the CIRP **25**(1): 359-361.

Boyd, S. and L. Vandenberghe (2004). Convex optimization, Cambridge Univ Pr.

Bronstein, A., M. Bronstein, M. Bronstein and R. Kimmel (2007). Numerical geometry of non-rigid shapes, Springer-Verlag New York Inc.

Bronstein, A., M. Bronstein and R. Kimmel (2006). "Generalized multidimensional scaling: a framework for isometry-invariant partial surface matching." Proceedings of the National Academy of Sciences **103**(5): 1168.

Bronstein, A., M. Bronstein and R. Kimmel (2007). "Efficient computation of isometry-invariant distances between surfaces." SIAM Journal on Scientific Computing **28**(5): 1812-1836.

Burago, D., Y. Burago and S. Ivanov (2001). A course in metric geometry.

Chen, F., G. M. Brown and M. Song (2000). "Overview of three-dimensional shape measurement using optical methods." Optical Engineering **39**: 10.

Chen, J. and Y. Liu (2011). "Locally linear embedding: a survey." Artificial Intelligence Review **36**(1): 29-48.

Chen, X. and F. Schmitt (1992). Intrinsic surface properties from surface triangulation, Springer.

Cox, M. (2000). Multidimensional scaling, CRC Press.

De Leeuw, J. (2005). "Applications of convex analysis to multidimensional scaling."

de Medeiros, C. J., J. A. F. Costa and L. A. Silva (2011). A comparison of dimensionality reduction methods using topology preservation indexes. Intelligent Data Engineering and Automated Learning-IDEAL 2011, Springer**:** 437-445.

Demartines, P. and J. Hérault (1997). "Curvilinear component analysis: A self-organizing neural network for nonlinear mapping of data sets." Neural Networks, IEEE Transactions on **8**(1): 148-154.

Dijkstra, E. (1959). "A note on two problems in connexion with graphs." Numerische mathematik **1**(1): 269-271.

Elad, A. and R. Kimmel (2003). "On bending invariant signatures for surfaces." IEEE Transactions on pattern analysis and machine intelligence **25**(10): 1285-1295.

Elbaz, A. and R. Kimmel (2003). "On bending invariant signatures for surfaces." IEEE Transactions on pattern analysis and machine intelligence **25**(10): 1285-1295.

Gao, J., N. Gindy and X. Chen (2006). "An automated GD&T inspection system based on non-contact 3D digitization." International Journal of Production Research **44**(1): 117-134.

Gentilini, I. and K. Shimada (2011). "Predicting and evaluating the post-assembly shape of thin-walled components via 3D laser digitization and FEA simulation of the assembly process." Computer-aided design **43**(3): 316-328.

Gersho, A. and R. M. Gray (1992). Vector quantization and signal compression, Kluwer Academic Pub.

Gower, J. C. (1966). "Some distance properties of latent root and vector methods used in multivariate analysis." Biometrika **53**(3-4): 325-338.

Greenspan, M. and G. Godin (2001). A nearest neighbor method for efficient ICP. 3-D Digital Imaging and Modeling, 2001. Proceedings. Third International Conference on, IEEE.

Holden, M. (2008). "A review of geometric transformations for nonrigid body registration." Medical Imaging, IEEE Transactions on **27**(1): 111-128.

Jaramillo, A., F. Prieto and P. Boulanger (2013). "Fast dimensional inspection of deformable parts from partial views." Computers in Industry.

Jaramillo, A., F. Prieto and P. Boulanger (2013). "Fixtureless inspection of deformable parts using partial captures." International Journal of Precision Engineering and Manufacturing **14**(1): 77-83.

Jolliffe, I. (2005). Principal component analysis, Wiley Online Library.

Kimmel, R. and J. Sethian (1998). "Computing geodesic paths on manifolds." Proc. Natl. Acad. Sci. USA **95**(15): 8431–8435.

Kohonen, T. (1982). "Self-organized formation of topologically correct feature maps." Biological cybernetics **43**(1): 59-69.

Kruskal, J. B. (1964). "Multidimensional scaling by optimizing goodness of fit to a nonmetric hypothesis." Psychometrika **29**(1): 1-27.

Lartigue, C., F. Theibaut, P. Bourdet and N. Anwar (2006). "DIMENSIONAL METROLOGY OF FLEXIBLE PARTS: IDENTIFICATION OF GEOMETRICAL DEVIATIONS FROM OPTICAL MEASUREMENTS." Advanced mathematical & computational tools in metrology VII: 196.

Lee, J. A., A. Lendasse and M. Verleysen (2002). Curvilinear distance analysis versus isomap. Proceedings of ESANN.

Lee, J. A. and M. Verleysen (2007). Nonlinear dimensionality reduction, Springer.

Li, Y. and P. Gu (2004). "Free-form surface inspection techniques state of the art review." Computer-Aided Design **36**(13): 1395-1417.

Li, Y. and P. Gu (2005). "Inspection of free-form shaped parts." Robotics and Computer-Integrated Manufacturing **21**(4-5): 421-430.

Maimon, O. Z. and L. Rokach (2005). Data mining and knowledge discovery handbook, Springer.

Mao, J. and A. K. Jain (2002). "Artificial neural networks for feature extraction and multivariate data projection." Neural Networks, IEEE Transactions on **6**(2): 296-317.

Mémoli, F. (2008). Gromov-Hausdorff distances in Euclidean spaces.

Mémoli, F. and G. Sapiro (2005). "A theoretical and computational framework for isometry invariant recognition of point cloud data." Foundations of Computational Mathematics **5**(3): 313-347.

Munoz, D., N. Vandapel and M. Hebert (2008). Directional associative markov network for 3-d point cloud classification, Citeseer.

Myronenko, A., X. Song and M. Carreira-Perpinán (2007). "Non-rigid point set registration: Coherent Point Drift." Advances in Neural Information Processing Systems **19**: 1009.

Radvar-Esfahlan, H. and S. A. Tahan (2010). Nonrigid geometric inspection using intrinsic geometry. Proceedings of The Canadian Society for Mechanical Engineering Forum 2010. Victoria, British Columbia.

Radvar-Esfahlan, H. and S. A. Tahan (2011). "Distance preserving dimensionality reduction methods and their applications in geometric inspection of nonrigid parts." 5th SASTECH Conference, Iran.

Radvar-Esfahlan, H. and S. A. Tahan (2011). "Nonrigid Geometric Metrology using Generalized Numerical Inspection Fixtures." Precision Engineering **36**(1): 1-9.

Ravishankar, S., H. Dutt and B. Gurumoorthy (2010). "Automated inspection of aircraft parts using a modified ICP algorithm." The International Journal of Advanced Manufacturing Technology **46**(1): 227-236.

Roweis, S. T. and L. K. Saul (2000). "Nonlinear dimensionality reduction by locally linear embedding." Science **290**(5500): 2323-2326.

Rusinkiewicz, S. and M. Levoy (2001). Efficient variants of the ICP algorithm, Citeseer.

Sabri, V., S. A. Tahan, T. Pham, H. Radvar-Esfahlan, B. Louhichi, M. Tahvilian and J. Bigeon (2013). FIXTURELESS PROFILE INSPECTION OF NON-RIGID PARTS. CIE43 Proceedings, 16-18 October 2013, The University of Hong Kong. Hong Kong.

Sammon Jr, J. W. (1969). "A nonlinear mapping for data structure analysis." Computers, IEEE Transactions on **100**(5): 401-409.

Savio, E., L. De Chiffre and R. Schmitt (2007). "Metrology of freeform shaped parts." CIRP Annals-Manufacturing Technology **56**(2): 810-835.

Schwartz, E., A. Shaw and E. Wolfson (1989). "A numerical solution to the generalized mapmaker's problem: flattening nonconvex polyhedral surfaces." IEEE Transactions on pattern analysis and machine intelligence **11**(9): 1005-1008.

Sethian, J. (1996). "A fast marching level set method for monotonically advancing fronts." Proceedings of the National Academy of Sciences **93**(4): 1591.

Sethian, J. (1999). Level set methods and fast marching methods, Cambridge university press Cambridge.

Sethian, J. (2008). "Theory, algorithms, and applications of level set methods for propagating interfaces." Acta numerica **5**: 309-395.

Shapovalov, R. and A. Velizhev "Cutting-Plane Training of Non-associative Markov Network for 3D Point Cloud Segmentation."

Shi, Q. and N. Xi (2008). "Automated data processing for a rapid 3D surface inspection system." IEEE International Conference on Robotics and Automation,3939-3944.

Shi, Q., N. Xi, Y. Chen and W. Sheng "Registration of Point Clouds for 3D Shape Inspection." Intelligent robots and systems, 2006 IEEE/RSJ 235-240.

Shiu, B., D. Ceglarek and J. Shi (1997). "Flexible beam-based modeling of sheet metal assembly for dimensional control." TRANSACTIONS-NORTH AMERICAN MANUFACTURING RESEARCH INSTITUTION OF SME: 49-54.

Sun, X., P. L. Rosin, R. R. Martin and F. C. Langbein (2008). Noise in 3D laser range scanner data, IEEE.

Tenenbaum, J. B., V. De Silva and J. C. Langford (2000). "A global geometric framework for nonlinear dimensionality reduction." Science **290**(5500): 2319-2323.

Torgerson, W. S. (1952). "Multidimensional scaling: I. Theory and method." Psychometrika **17**(4): 401-419.

Van der Maaten, L., E. Postma and H. Van den Herik (2009). "Dimensionality reduction: A comparative review." Journal of Machine Learning Research **10**: 1-41.

Vandenberghe, L. and S. Boyd (1996). "Semidefinite programming." SIAM review **38**(1): 49-95.

Weckenmann, A. and A. Gabbia (2005). Testing formed sheet metal part using fringe projection and evaluation by virtual distortion compensation. The 5th International Workshop on Automatic Processing of Fringe Patterns, Springer.

Weckenmann, A., J. Weickmann and N. Petrovic (2007). Shortening of inspection processes by virtual reverse deformation. 4th International Conference and Exhibition on Design and Production of Machines and Dies/Molds. Cesme, Turkey.

Weinberger, K. Q. and L. K. Saul (2004). Unsupervised learning of image manifolds by semidefinite programming. Computer Vision and Pattern Recognition, 2004. CVPR 2004. Proceedings of the 2004 IEEE Computer Society Conference on, IEEE.

Yang, M. and E. Lee (1999). "Segmentation of measured point data using a parametric quadric surface approximation." Computer-aided design **31**(7): 449-457.

Yin, H. (2007). "Nonlinear dimensionality reduction and data visualization: a review." International Journal of Automation and Computing **4**(3): 294-303.

Young, G. and A. S. Householder (1938). "Discussion of a set of points in terms of their mutual distances." Psychometrika **3**(1): 19-22.